PHYSICS OPPORTUNITIES AT ELECTRON-ION COLLIDERS

Anna Stasto

Penn State & RIKEN BNL & Cracow INP

Outline

What are open fundamental questions?

Exploring nuclear structure.

High parton density regime.

Initial conditions for AA collisions.

What measurements do we need?

Physics potential of LHeC and EIC.

Nuclear structure

Fundamental interaction is described by QCD in terms of quarks and gluons as elementary degrees of freedom.

$$\mathcal{L}_{\mathrm{QCD}} = -\frac{1}{4} F_{\mu\nu}^A F_A^{\mu\nu} + \sum_{\mathrm{flavours}} \bar{\Psi}_a (i\partial^\mu \gamma_\mu \delta_{ab} - g_s \gamma^\mu t_{ab}^C A_\mu^C - m_f \delta_{ab}) \Psi_b$$

$$F_{\mu\nu}^A = \partial_\mu A_\nu^A - \partial_\mu A_\nu^A - g f^{ABC} A_\mu^B A_\nu^C$$

High energy: larger transverse momenta involved. Quarks, gluons are explored at smaller distance scales.

What is the structure of the nucleus in terms of these fundamental degrees of freedom?

Nuclear structure

A classic way to measure the nuclear/hadron structure and quark/gluon distributions is through deep inelastic scattering.

Rutherford 1911 $\longrightarrow$ SLAC 1967 $\longrightarrow$ HERA 2007 $\longrightarrow$ EIC & LHeC ?

Deep Inelastic Scattering : $\quad \dfrac{d^2\sigma^{ep \to eX}}{dx\,dQ^2} = \dfrac{4\pi\alpha_{e.m.}^2}{xQ^4}\left[\left(1 - y + \dfrac{y^2}{2}\right)F_2(x,Q^2) - \dfrac{y^2}{2}F_L(x,Q^2)\right]$
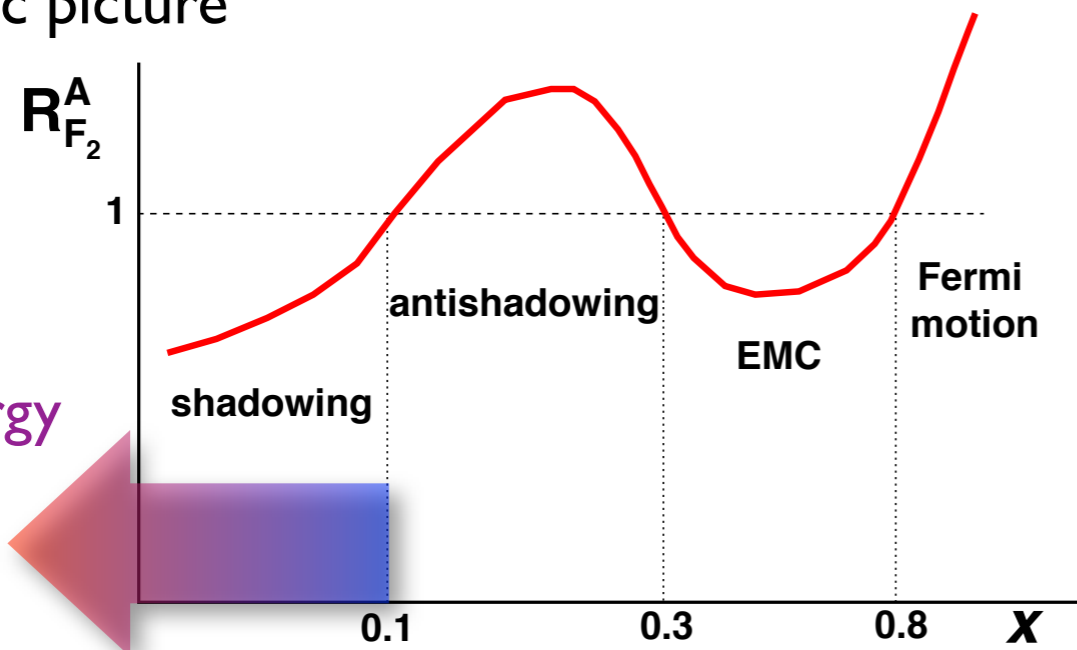
Nuclear ratio for structure function

$$R_{F_2}^A(x,Q^2) = \frac{F_2^A(x,Q^2)}{A\,F_2^{\mathrm{nucleon}}(x,Q^2)}$$

Nuclear effects $\qquad R^A \;\neq\; 1$
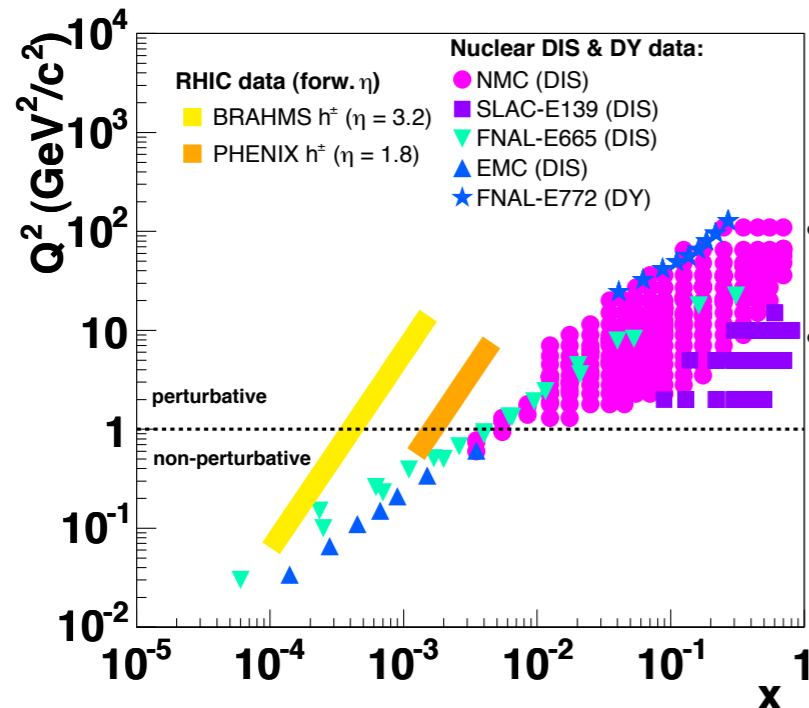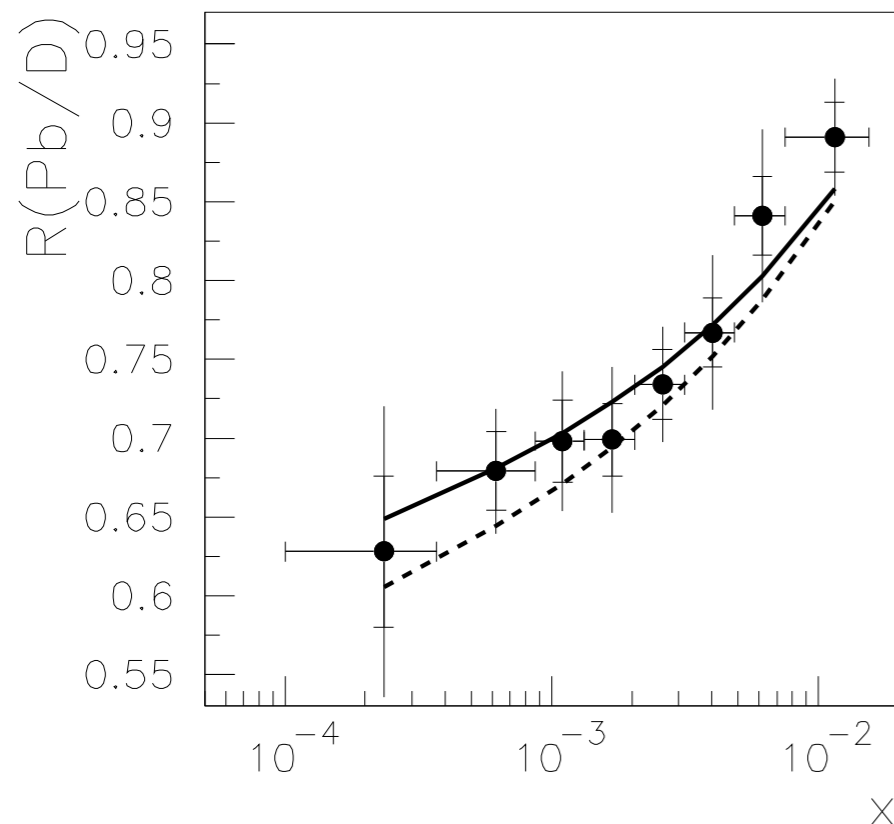
- Fermi motion $\quad x \geq 0.8$

- EMC region $\quad 0.25 - 0.3 \leq x \leq 0.8$

- Antishadowing region $\quad 0.1 \leq x \leq 0.25 - 0.3$

- Shadowing region $\quad x \leq 0.1$

Schematic picture

High energy

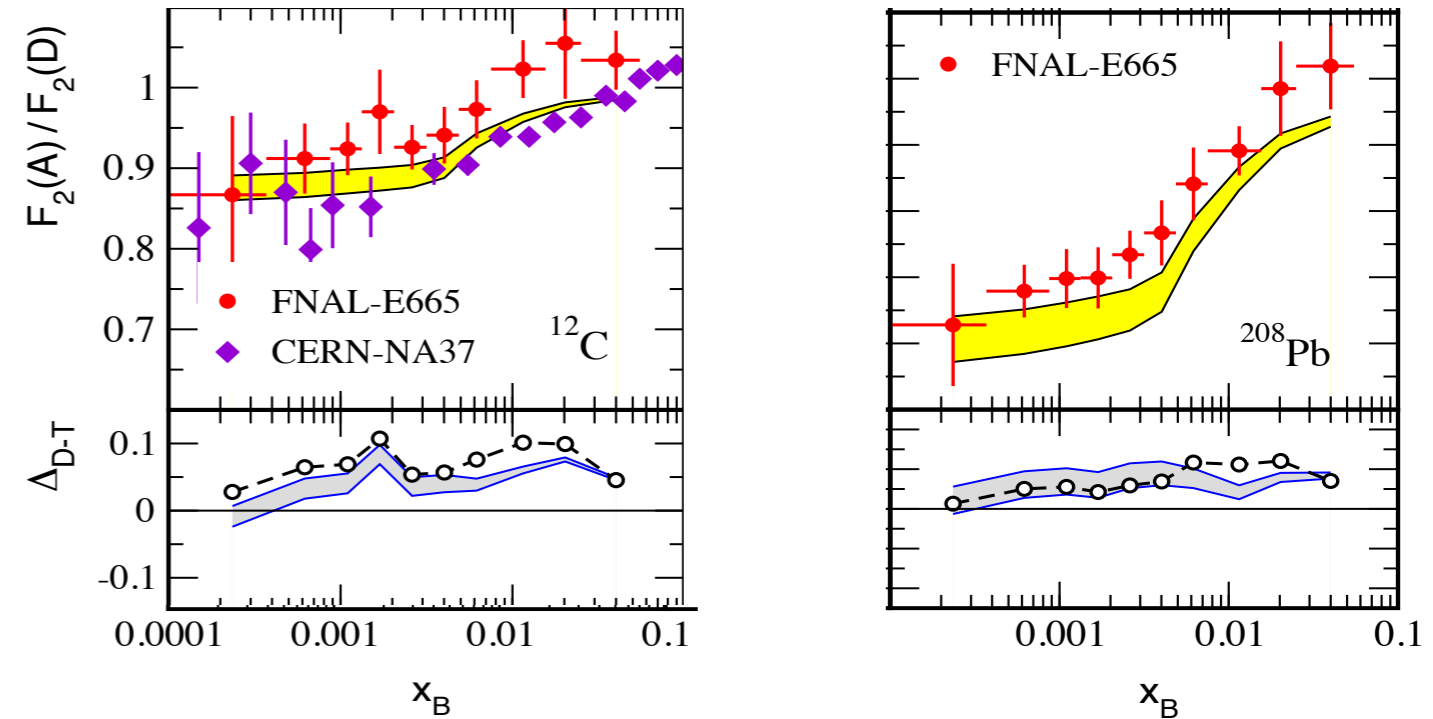# What the nuclear DIS data tell us?

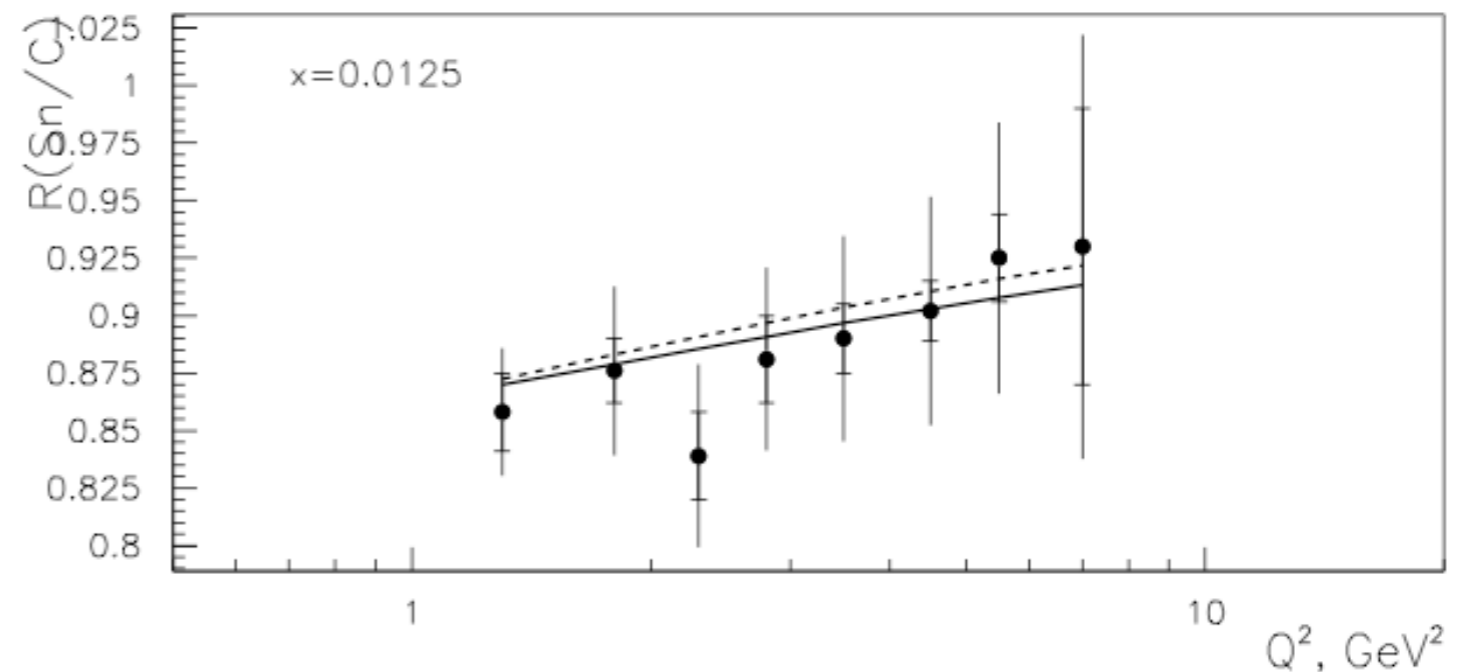## Kinematic coverage in nuclear DIS and DY

Shadowing increases with A

Shadowing increases with decreasing x

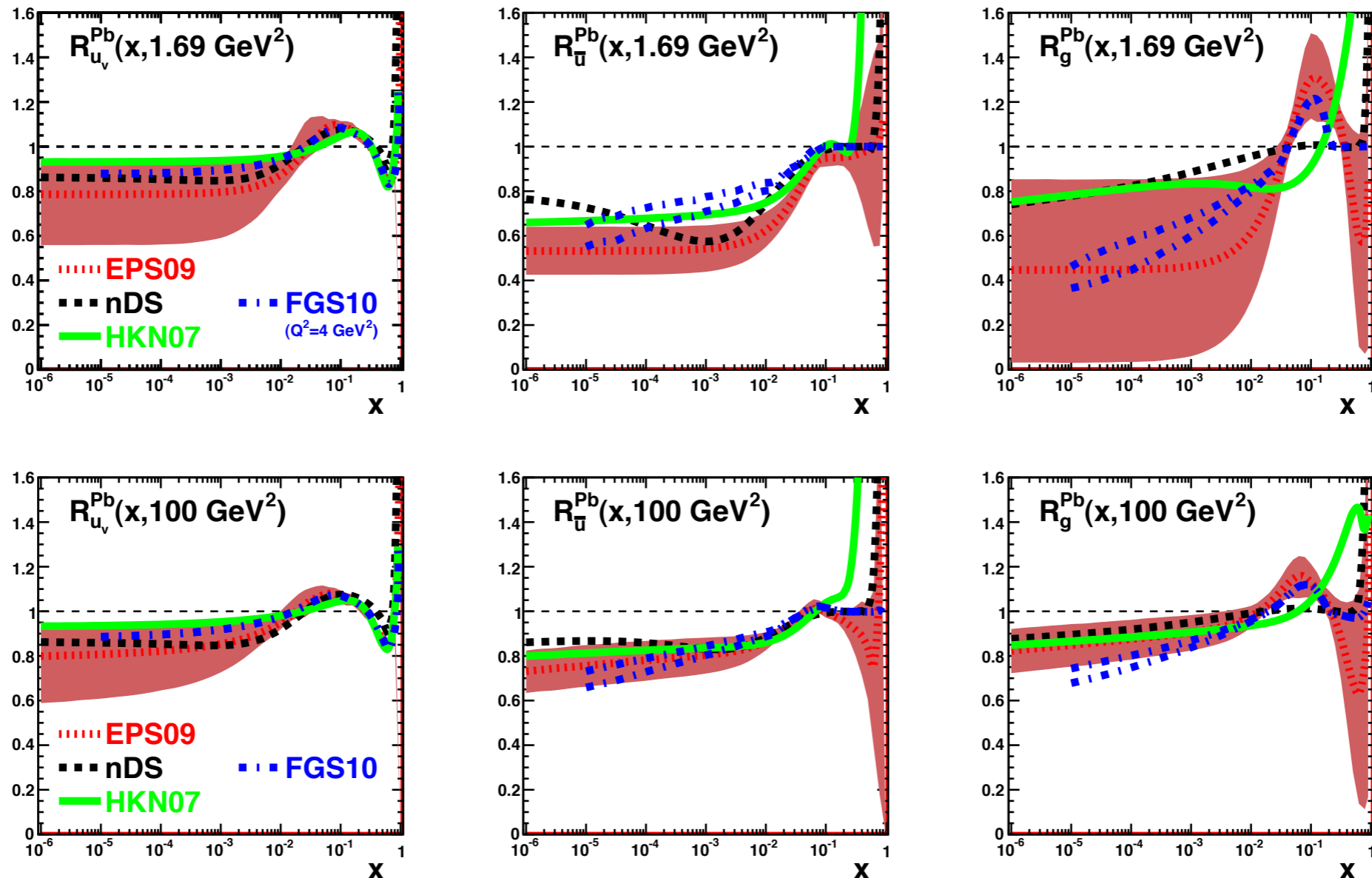## Shadowing decreases with increasing Q

From structure functions to pdfs

Collinear factorization in DIS:

$$F_{2,L}^{A}(x, Q^2) = C_i(\alpha_s; x, Q^2/\mu^2) \otimes x f_i^{A}(x, \mu^2)$$

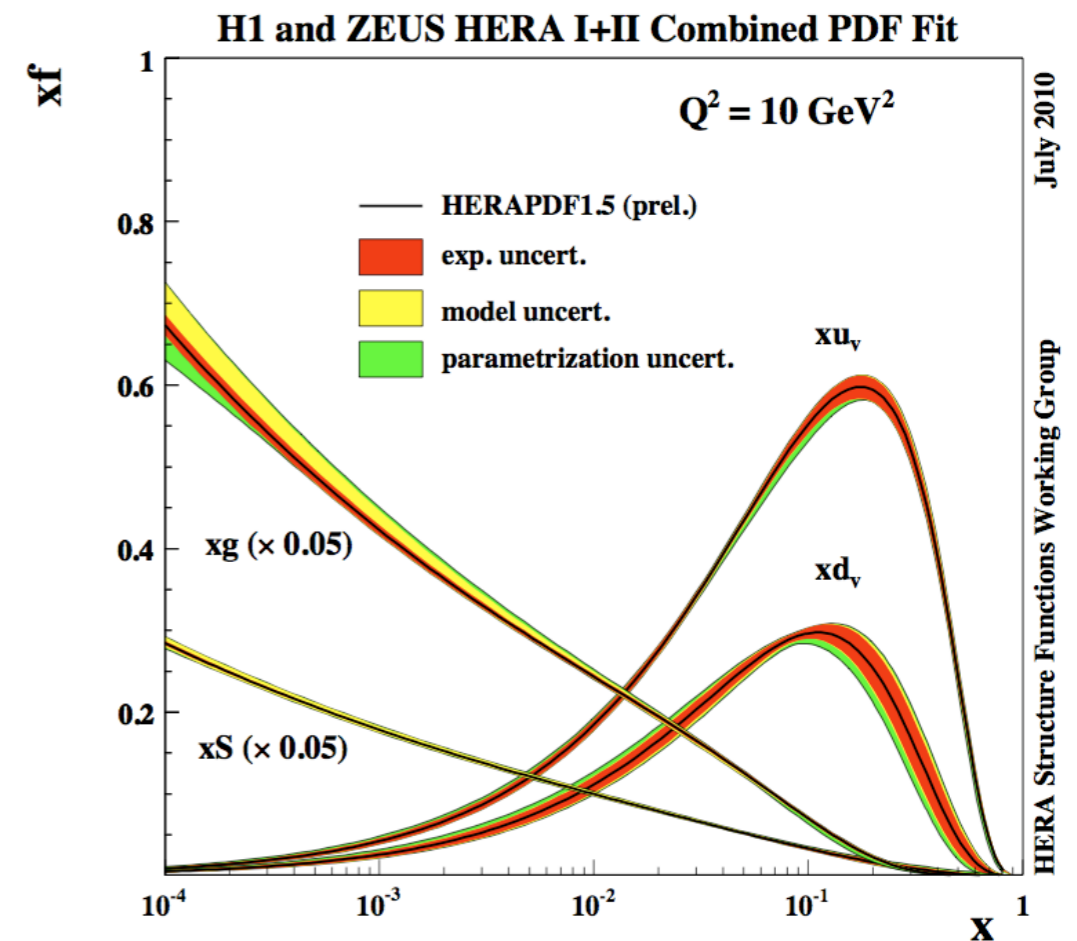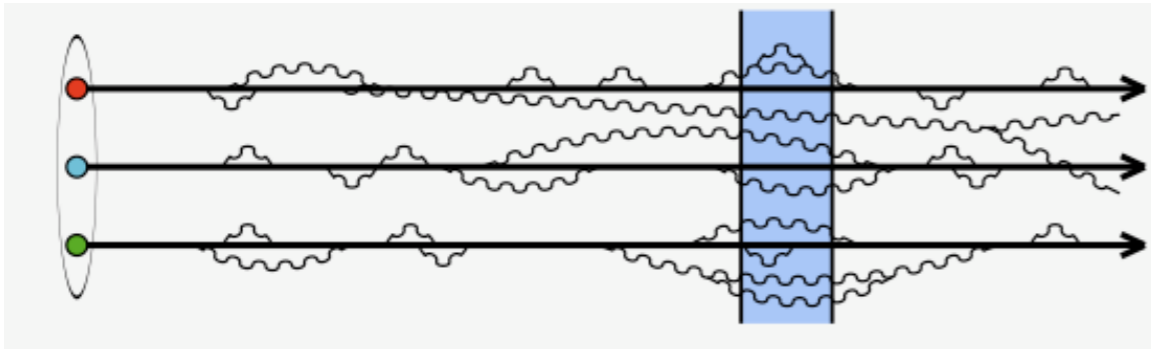Current uncertainties of the parton distribution in nuclei

Large uncertainty at small values of x especially in the gluon and sea quark sector

Proton case: gluon density at small x

Observation from electron-proton collider HERA: Gluon density dominates at small x.

Hadron at large energy

Increasing number of fluctuations at high energy/small x.

- Rise of the cross sections with energy.
- Bulk of the particle production (multiplicities).
- Many body dense system. New emergent phenomena expected. New degrees of freedom.

Small x: high parton density

- At small x the linear evolution gives strongly rising gluon density.

- Non-linear parton evolution includes the recombination effects of gluons.

- Dynamically generated momentum scale:


Fast proton or nucleus

Saturation scale: $Q_s^2(x)$

- Characterizes the boundary between the non-linear and linear regime.

- Increases with energy or with decreasing x.
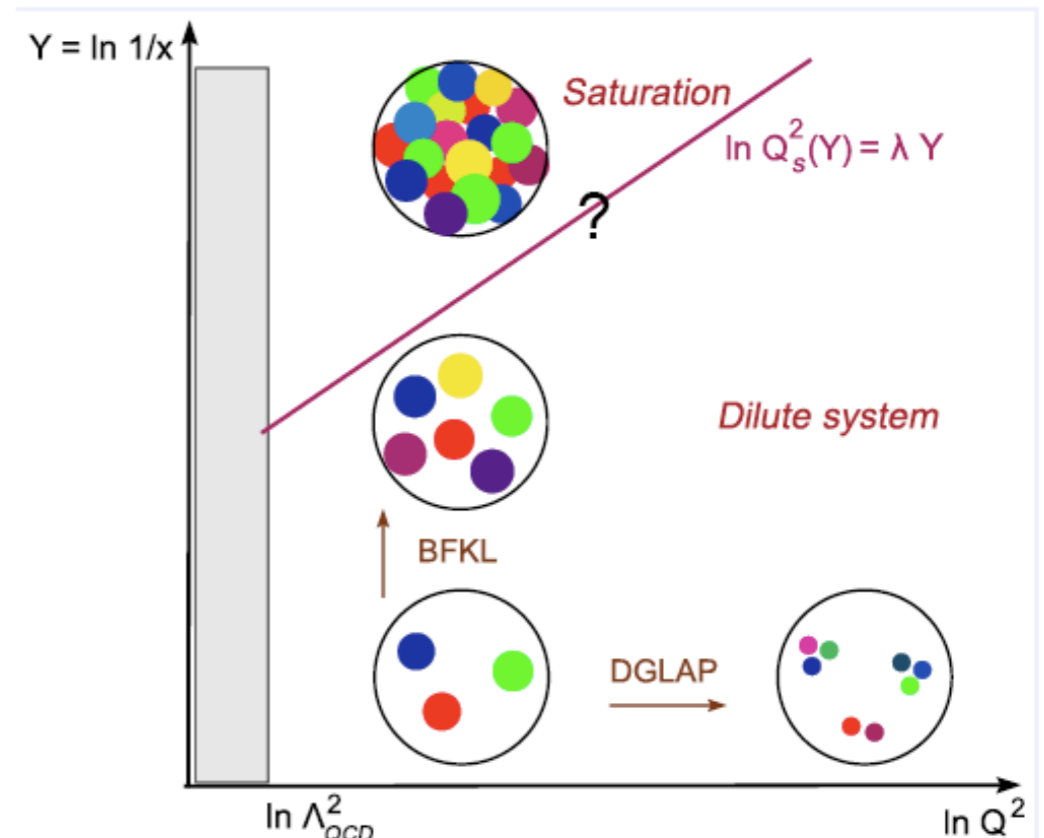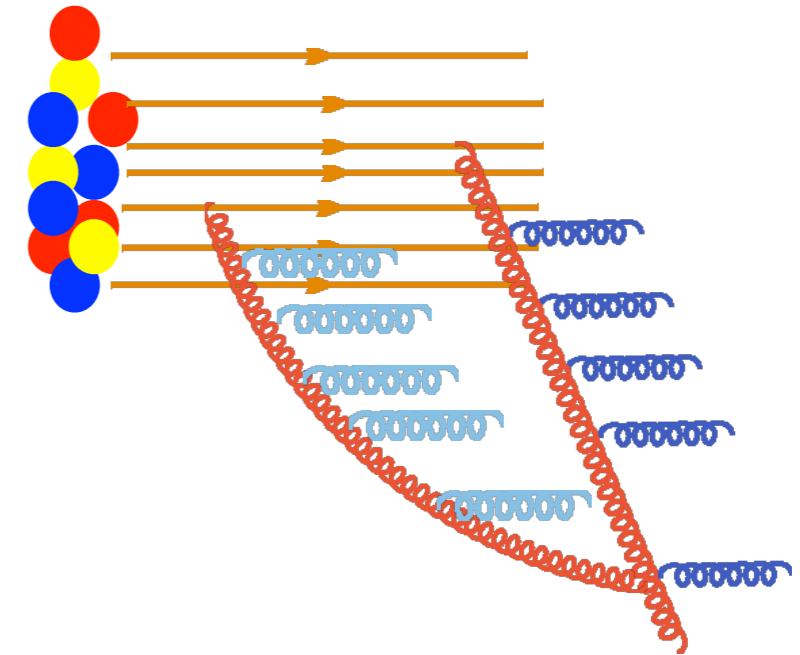
Saturation scale grows with A

- Probes interact over distances $L \sim \dfrac{1}{2 m_N x}$

- For $L > 2 R_A \sim A^{1/3}$ high-energy probes interact coherently across nuclear size. Very large field strengths.

color charges at large x

small x gluon

R ~ A^1/3
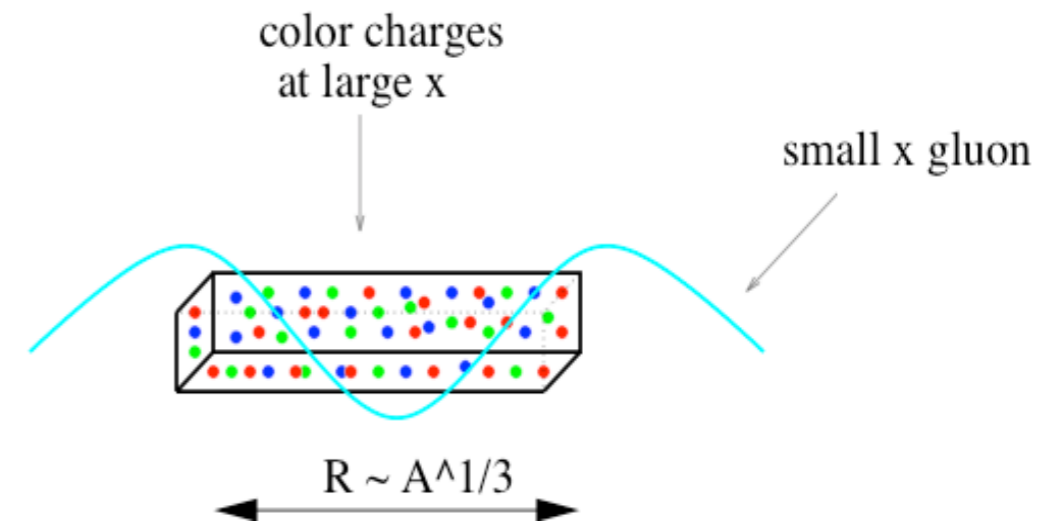
Scattering off nuclei: Saturation is reached for smaller energies due to the enhancement from A.
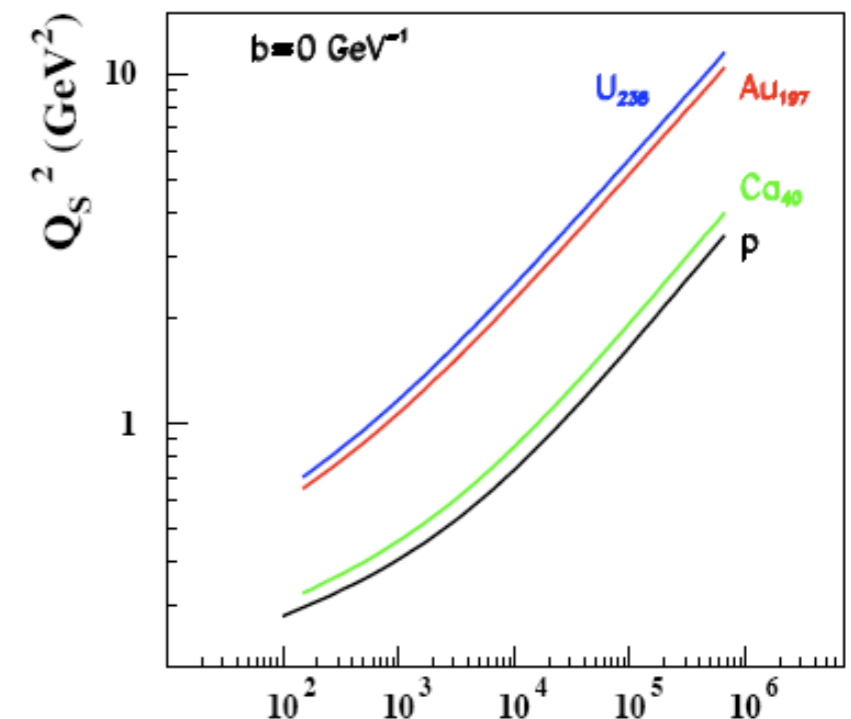
$$Q_s^2(x, A) \sim Q_0^2 \, x^{-\lambda} A^{1/3}$$

Nuclei at high energy

Kowalski, Teaney

Large A and small x

High parton densities.
New regime of QCD

Nuclear structure

In order to unfold the details of the nuclear structure less integrated distributions are needed. For the better understanding of the more exclusive final states need extra information about transverse position or momenta of partons.

- Impact parameter profile of nucleus. Generalized parton distributions.
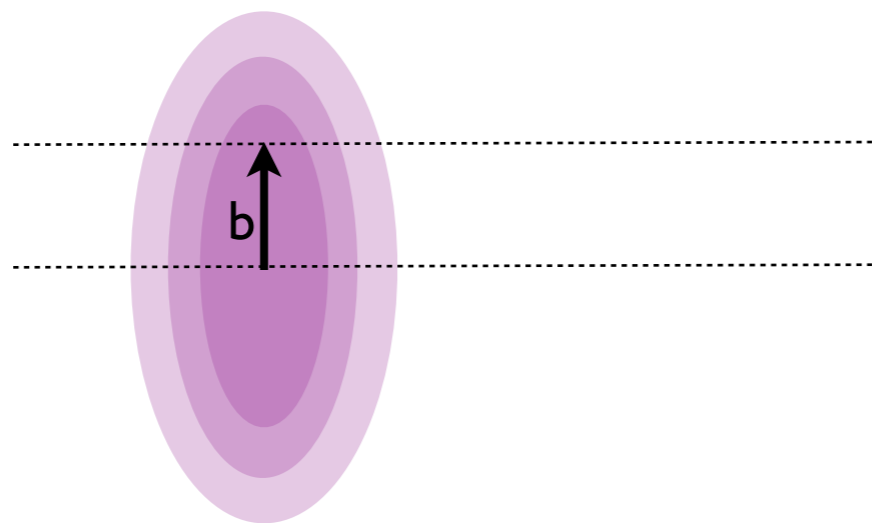
Momentum transfer

$$q(x, \mathbf{b}; \mu) = \int \frac{d^2\mathbf{q}}{(2\pi)^2} e^{-i\mathbf{b}\cdot\mathbf{q}} H^q(x, \xi = 0, t = -\mathbf{q}^2; \mu)$$

Probability of finding a quark with light cone fraction x at impact parameter b.
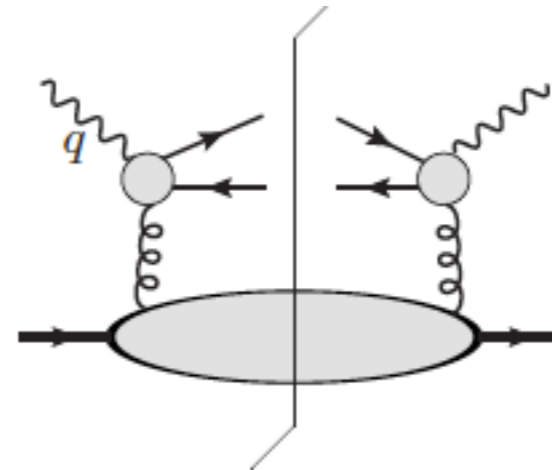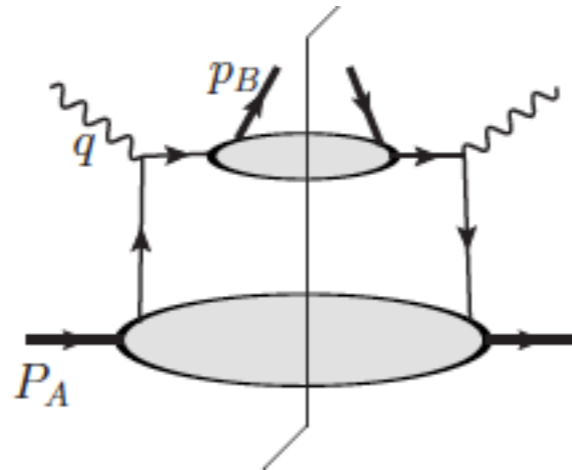
Transverse spatial distribution is a fundamental characteristic of nucleon/ nucleus: Gribov diffusion, chiral dynamics, issues of saturation at small x

$$Q_s(x, \mathbf{b})$$

Exploring nuclear structure

Unintegrated/transverse momentum dependent parton distributions.

SIDIS

Heavy Quark production

$$\frac{d\sigma}{dx\,dQ^2\,dz\,d^2\boldsymbol{P}_{B\perp}} = \sum_j \int d^2\boldsymbol{k}_\perp\, H_j f_{j/A}(x,\boldsymbol{k}_\perp) d_{B/j}(z, \boldsymbol{p}_{B\perp} + z\boldsymbol{k}_\perp), \qquad 4M^2\sigma_{\gamma g}(\rho, M^2/Q_0^2) = \int d^2\boldsymbol{k}_\perp \int_0^1 \frac{dz}{z}\hat{\sigma}(\rho/z, \boldsymbol{k}_\perp^2/M^2) f_{g/h}(x,\boldsymbol{k}_\perp),$$

Contain information about the transverse momentum distribution. Useful for more exclusive final states, SIDIS, heavy quark production, dijet production, forward jets.
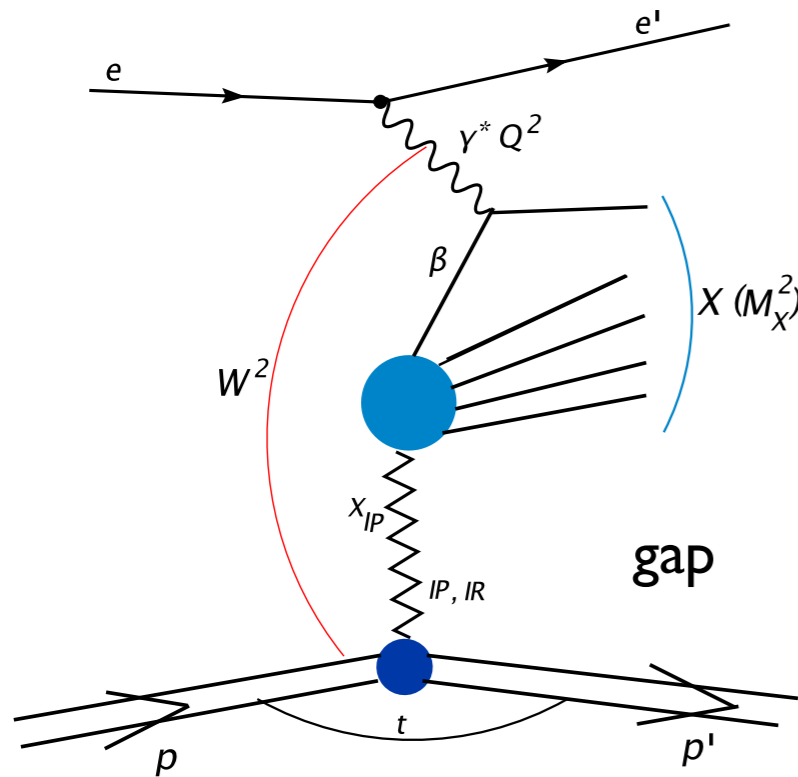
Example: dijet production in DIS, angular decorrelation between jets.
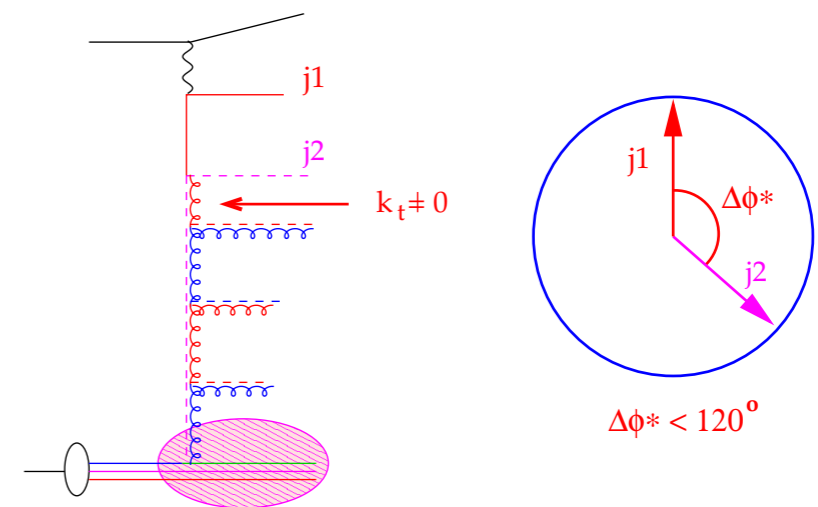
Decorrelation of jets at small x due to the increased transverse momentum. Sensitivity to nonlinear evolution when $k_T \sim Q_s(A, x)$

Diffraction in ep

$$e + p \rightarrow e' + p' + X$$

Proton stays intact and separated by a rapidity gap

M^2 diffractive mass

$t = (p - p')^2$ momentum transfer

$\Delta \eta = \ln 1/x_{I\!\!P}$ Rapidity gap

$$x_{I\!\!P} = \frac{Q^2 + M^2 - t}{Q^2 + W^2}$$ momentum fraction of the Pomeron with respect to the hadron
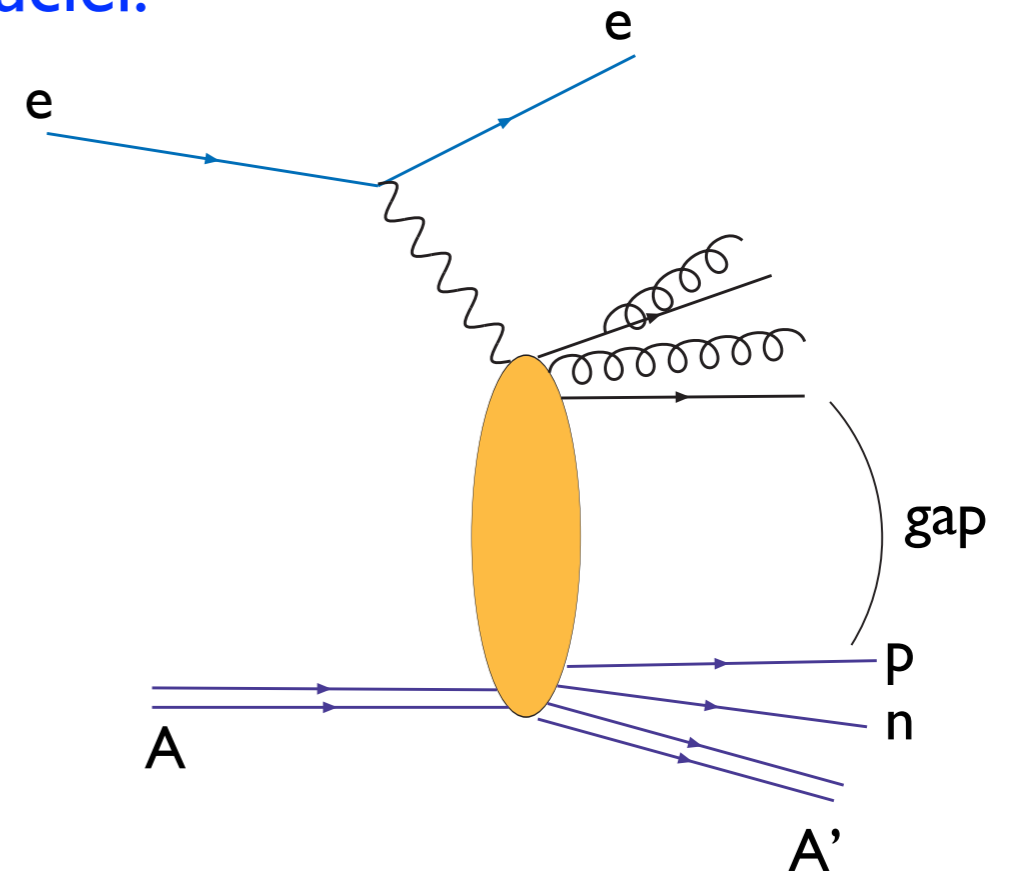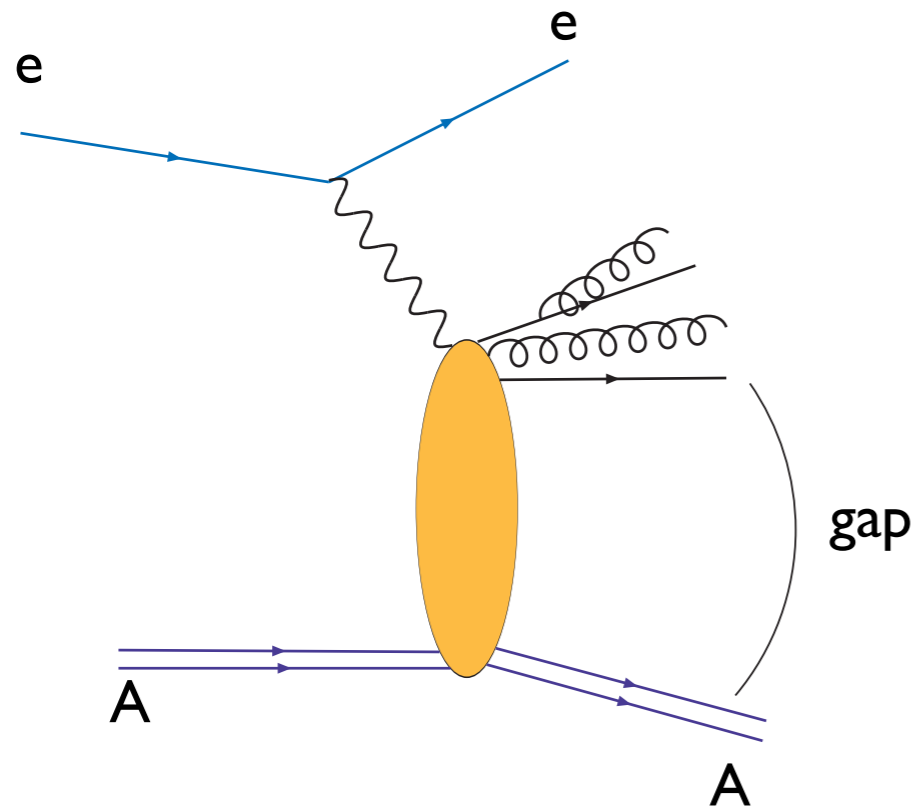
$$\beta = \frac{Q^2}{Q^2 + M^2 - t}$$ momentum fraction of the struck parton with respect to the Pomeron

$$x = x_{I\!\!P}\, \beta$$ Bjorken x

Diffraction in eA

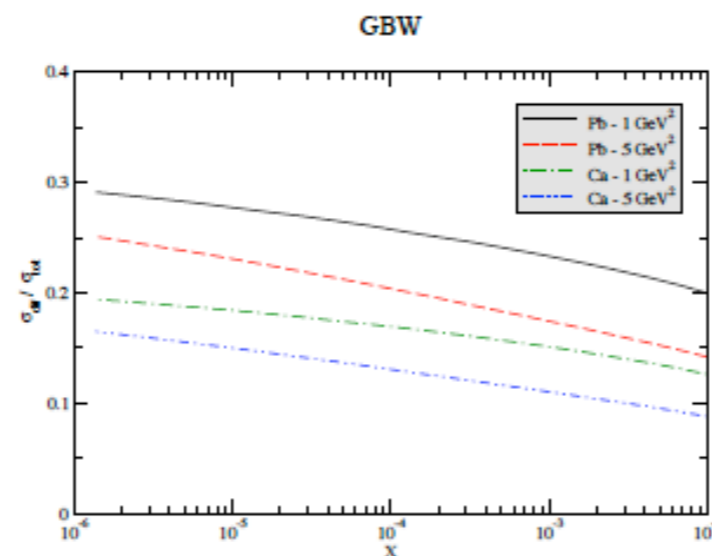Two possibilities for the diffractive events in nuclei:
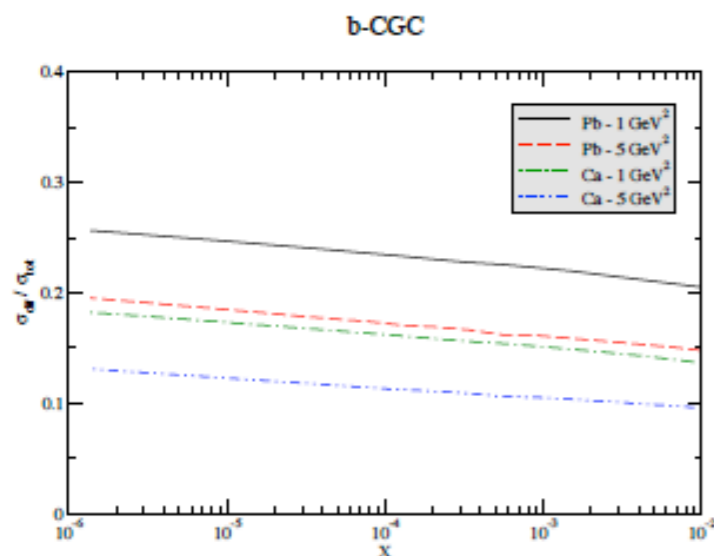

Coherent: No-breakup

Incoherent: With breakup into nucleons
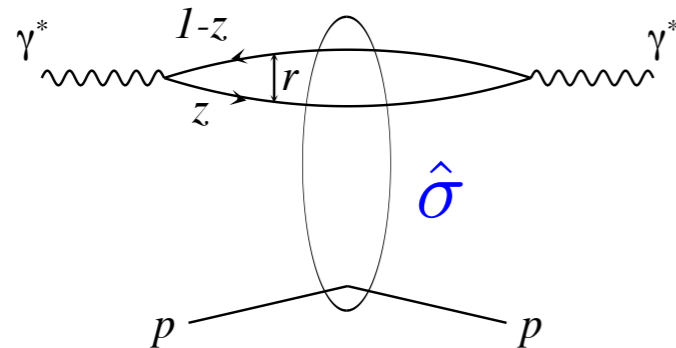The gap is still there

Diffractive to inclusive ratio in eA

Predictions give
20%-40% for $\sigma_{\mathrm{diff}}/\sigma_{\mathrm{tot}}$
in the regime down
to 10^{-6}

Diffraction, dipole models and saturation

$$\sigma_L = \frac{\alpha_{em}}{\pi} \sum_f e_f^2 \int d^2\mathbf{r} \int_0^1 dz\, 4\, Q^2\, z^2(1-z)^2\, K_0^2(Qr)$$

$$\times \int \frac{d^2\mathbf{l}}{l^4}\, \alpha_s f(x, l^2)\, (1 - e^{-i\mathbf{l}\cdot\mathbf{r}})\, (1 - e^{i\mathbf{l}\cdot\mathbf{r}}),$$

Dipole model for the description of DIS at high energy: photon fluctuates into qqbar pair of size **r** and undergoes an interaction with the target
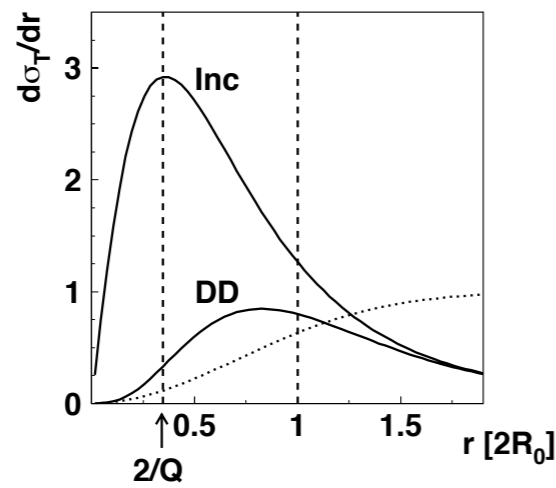
Figure 3.1: *Schematic representation of the basic factorization in inclusive DIS at small*

$$\sigma_{T,L}(x, Q^2) = \int d^2\mathbf{r} \int_0^1 dz \sum_f |\Psi_{T,L}^f(\mathbf{r}, z, Q^2)|^2 \, \hat{\sigma}(x, \mathbf{r}).$$

where the *photon wave functions* $\Psi_{T,L}^f$ describe the splitting of the virtual photon into the $q\bar{q}$ pair [92],

$$|\Psi_T^f(\mathbf{r}, z, Q^2)|^2 = \frac{3\,\alpha_{em}}{2\pi^2}\, e_f^2 \left\{ [z^2 + (1-z)^2]\, Q^2\, K_1^2(Qr) + m_f^2 K_0^2(Qr) \right.$$

Inclusive: dominated by relatively hard component
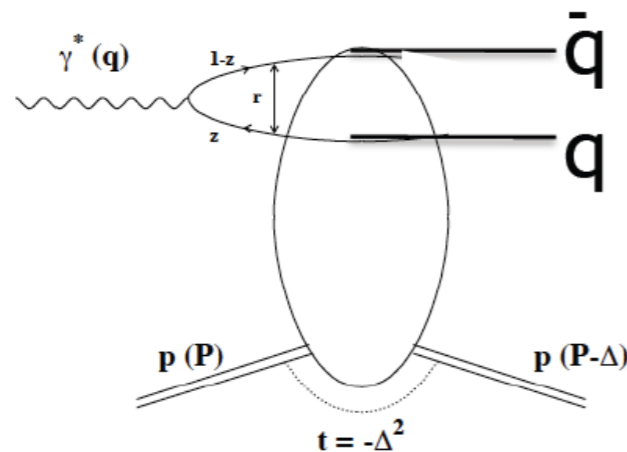
$$\frac{d\sigma_{T,L}^D}{dt}\bigg|_{t=0} = \frac{1}{16\pi} \int d^2\mathbf{r}\, dz \sum_f |\Psi_{T,L}^f(\mathbf{r}, z)|^2\, \hat{\sigma}^2(x, \mathbf{r})$$

and Q is defined in eq. (3.3). Formula (3.7) forms the basis of the following analysis.

Diffractive: dominated by the semi-hard momenta

$$\times \int \frac{d^2\mathbf{l}}{l^4}\, \alpha_s f(x, l^2)\, (1 - e^{-i\mathbf{l}\cdot\mathbf{r}})\, (1 - e^{i\mathbf{l}\cdot\mathbf{r}}), \quad (3.6)$$

were $K_{0,1}$ are the Bessel–Mc Donald functions. Both cross sections can be written in the following compact form [90, 36], shown schematically in Fig. 3.1,

$$\sigma_{T,L}(x, Q^2) = \int d^2\mathbf{r} \int_0^1 dz \sum_f |\Psi_{T,L}^f(\mathbf{r}, z, Q^2)|^2\, \hat{\sigma}(x, \mathbf{r}). \quad (3.7)$$

where the *photon wave functions* $\Psi_{T,L}^f$ describe the splitting of the virtual photon into the $q\bar{q}$ pair [92],

$$|\Psi_T^f(\mathbf{r}, z, Q^2)|^2 = \frac{3\,\alpha_{em}}{2\pi^2}\, e_f^2 \left\{ [z^2 + (1-z)^2]\, Q^2\, K_1^2(Qr) + m_f^2 K_0^2(Qr) \right\}, \quad (3.8)$$

overlap function in the dipole model
typical dipole sizes involved in the process

Diffraction

- Large distances: long range effects, correlations. Relation to saturation.

- Explore the Pomeron structure, color neutral excitations.

- t-dependence gives access to the impact parameter profile, especially in exclusive processes.

- Tests of factorization in diffraction, does it hold in eA in the same parameter range as in ep?

- Relation between diffraction in ep and shadowing in eA.
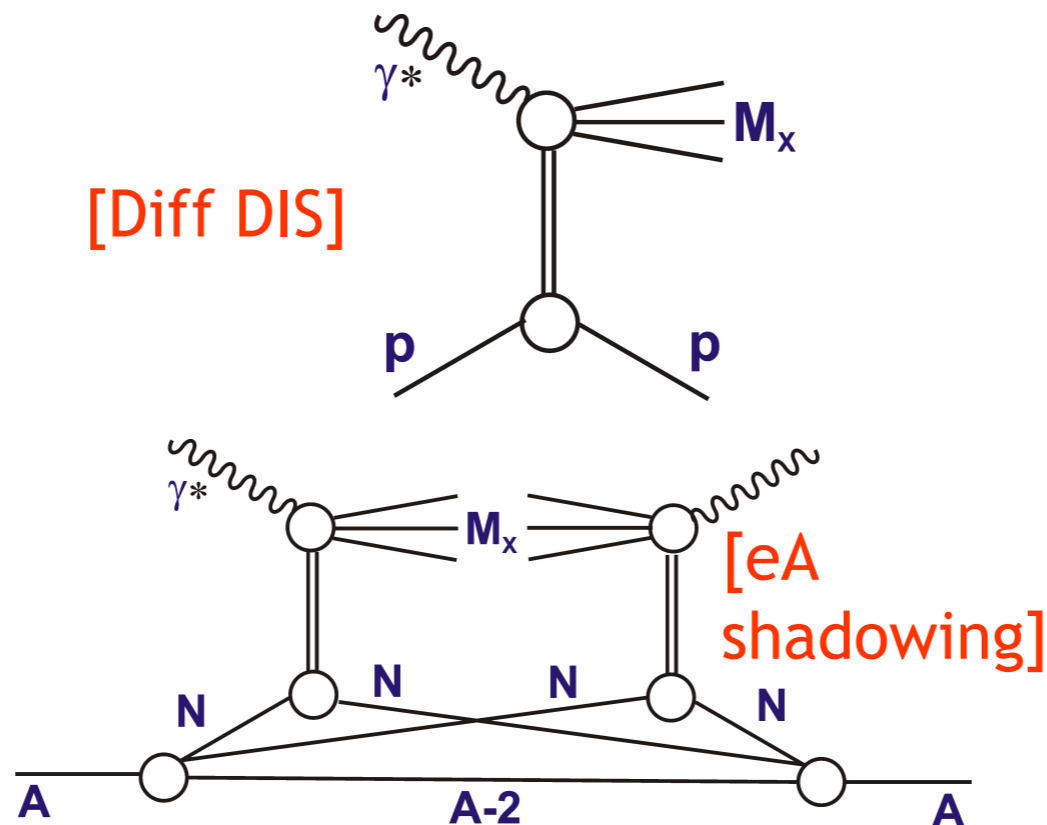
Importance of eA for AA
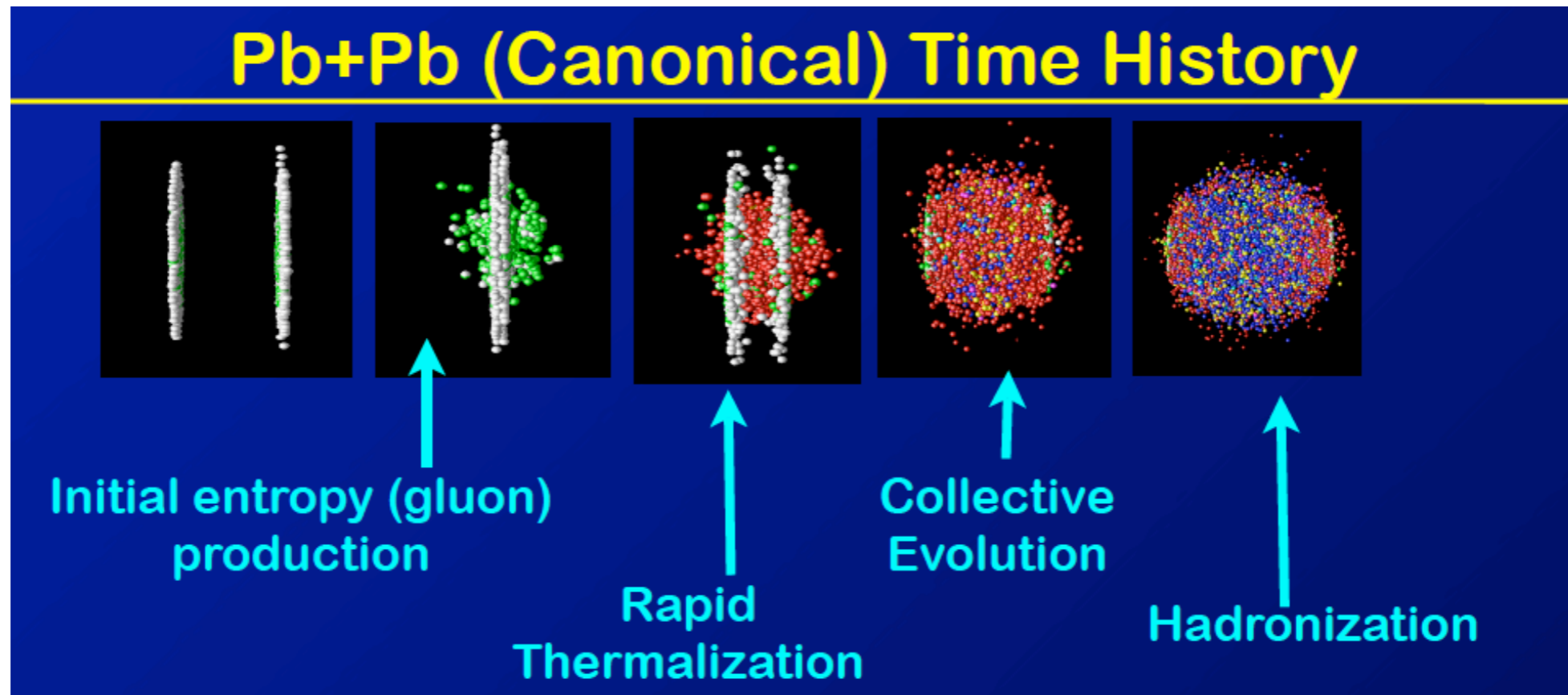
Understanding the initial conditions in AA is critical for the later evolution of the system.

Simulations based on the initial wave function with parton saturation describe fairly well the multiplicites at RHIC and LHC.

However, many free parameters, poor understanding of impact parameter dependence.

Need an independent measurement of the initial condition : eA.

Parton dynamics in nuclear medium

• A high energy eA collider would allow to study the dynamics of hadronization, testing the parton/hadron energy loss mechanism by introducing a length of colored material which would modify its pattern (length/nuclear size, chemical composition).

DIS in vacuum (in practice on a nucleon)
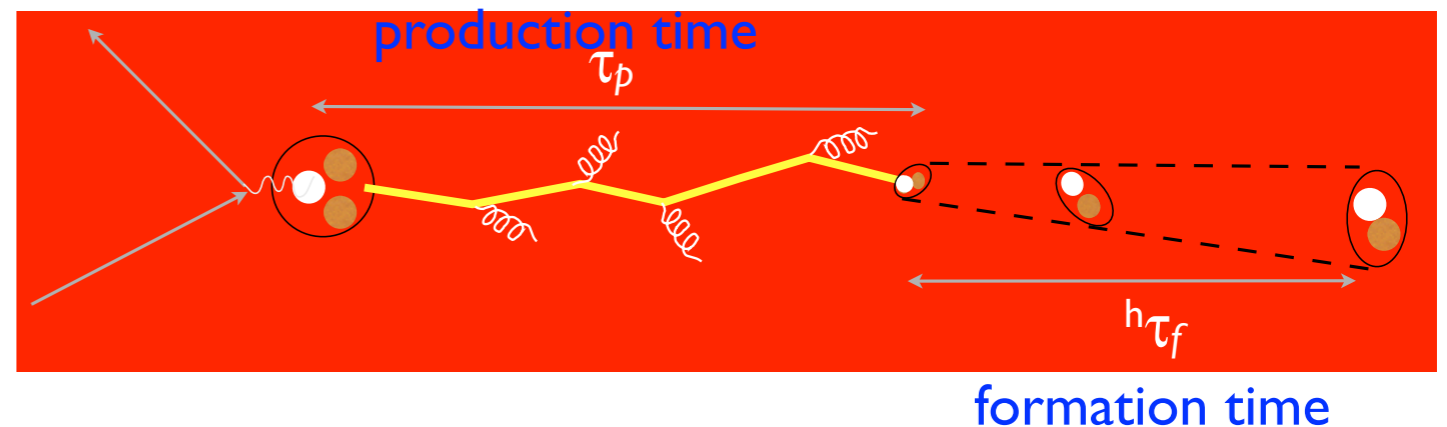
DIS in medium:

Hadron forms outside, high energy, partonic energy loss
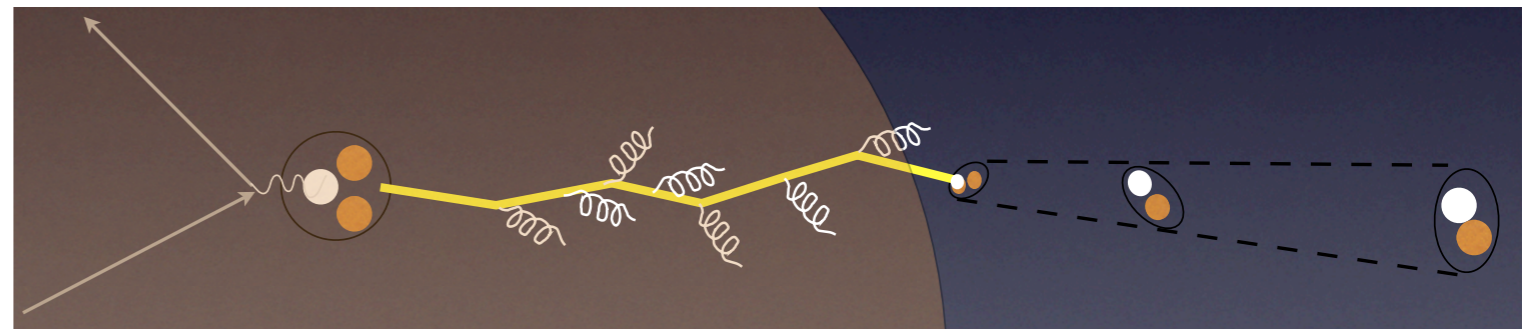
Hadron forms inside, low energy, prehadron(hadron) absorption.
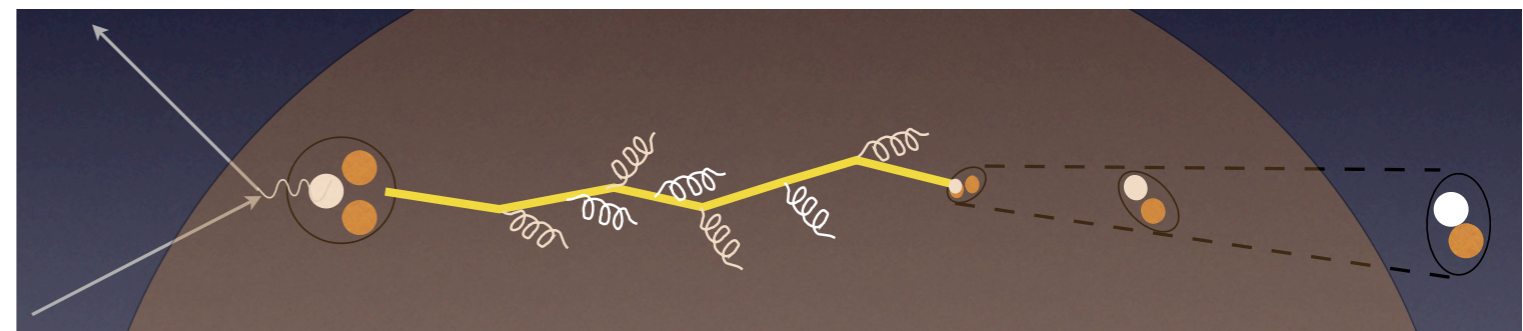
Connection between the transverse momentum broadening in SIDIS and the saturation scale which characterizes the dense medium. $\Delta p^2_T = Q^2_s(b,E)$

EIC & LHC
physics potential

Future DIS facilities

E_{cm} vs L

C: DIS with LHC beam

Project:
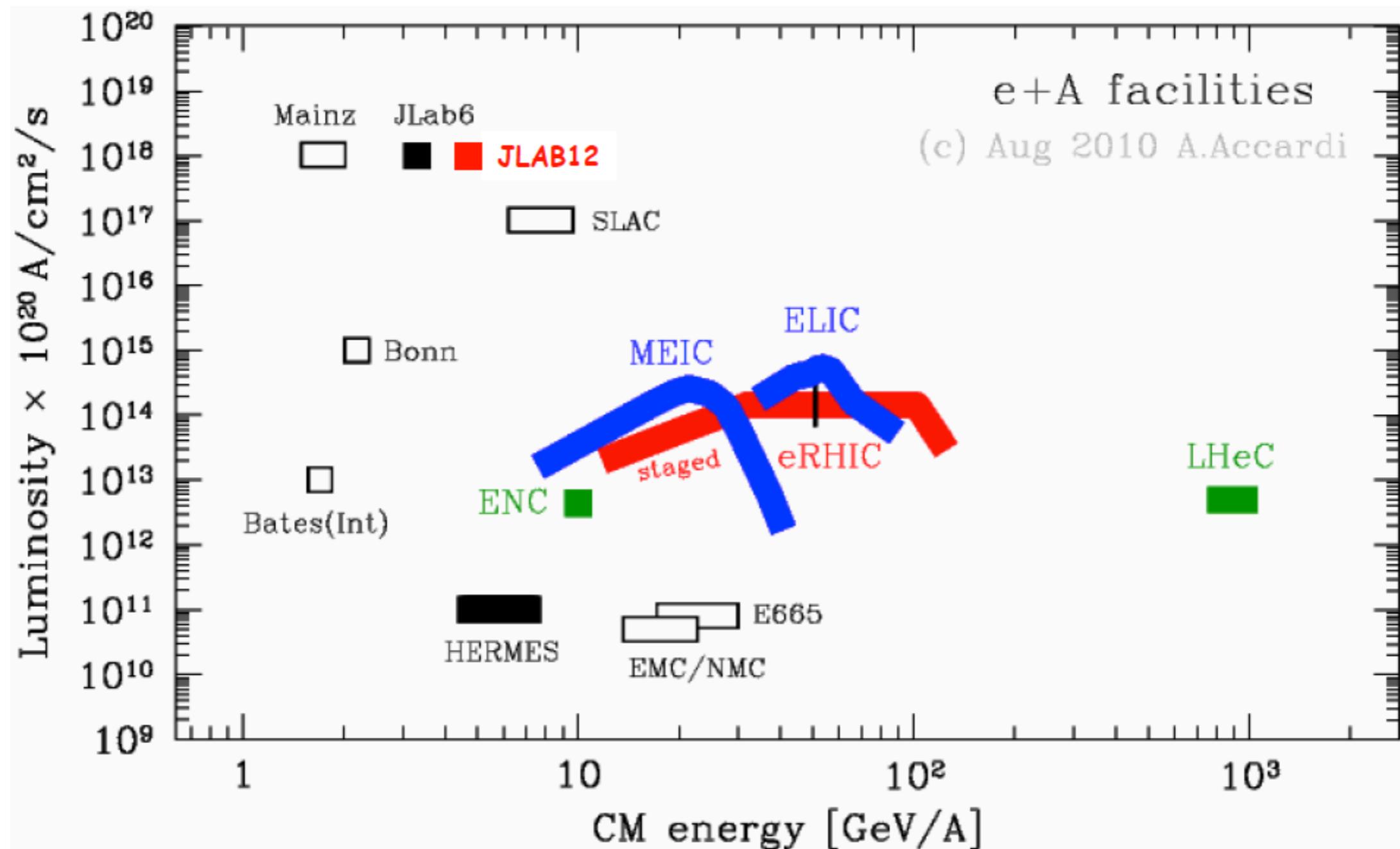
$$E_p = 7 \text{ TeV}$$

$$E_A = 2.75 \text{ TeV/nucleon}$$

Project:

$$E_e = 50 - 150 \text{ GeV}$$

ep/ea collisions

$$\sqrt{s} \simeq 1 - 2 \text{ TeV}$$

d'Enterria

- Requirements:

* Luminosity~10^{33} cm⁻²s⁻¹.   eA: L$_{en}$~10^{32} cm⁻²s⁻¹

* Acceptance: 1-179 degrees (low-x ep/eA).

* Tracking to 1 mrad.

* EMCAL calibration to 0.1 %.

* HCAL calibration to 0.5 %.

* Luminosity determination to 1 %.

* Compatible with LHC operation.

nuclear DIS - $F_{2,A}(x,Q^2)$

Proposed facilities:

LHeC

Fixed-target data:

NMC

E772

E139

E665

EMC

e-Pb (LHeC)
(70 GeV - 2.5 TeV)

Q_s^2 (Pb, b=0 fm)

perturbative

non-perturbative
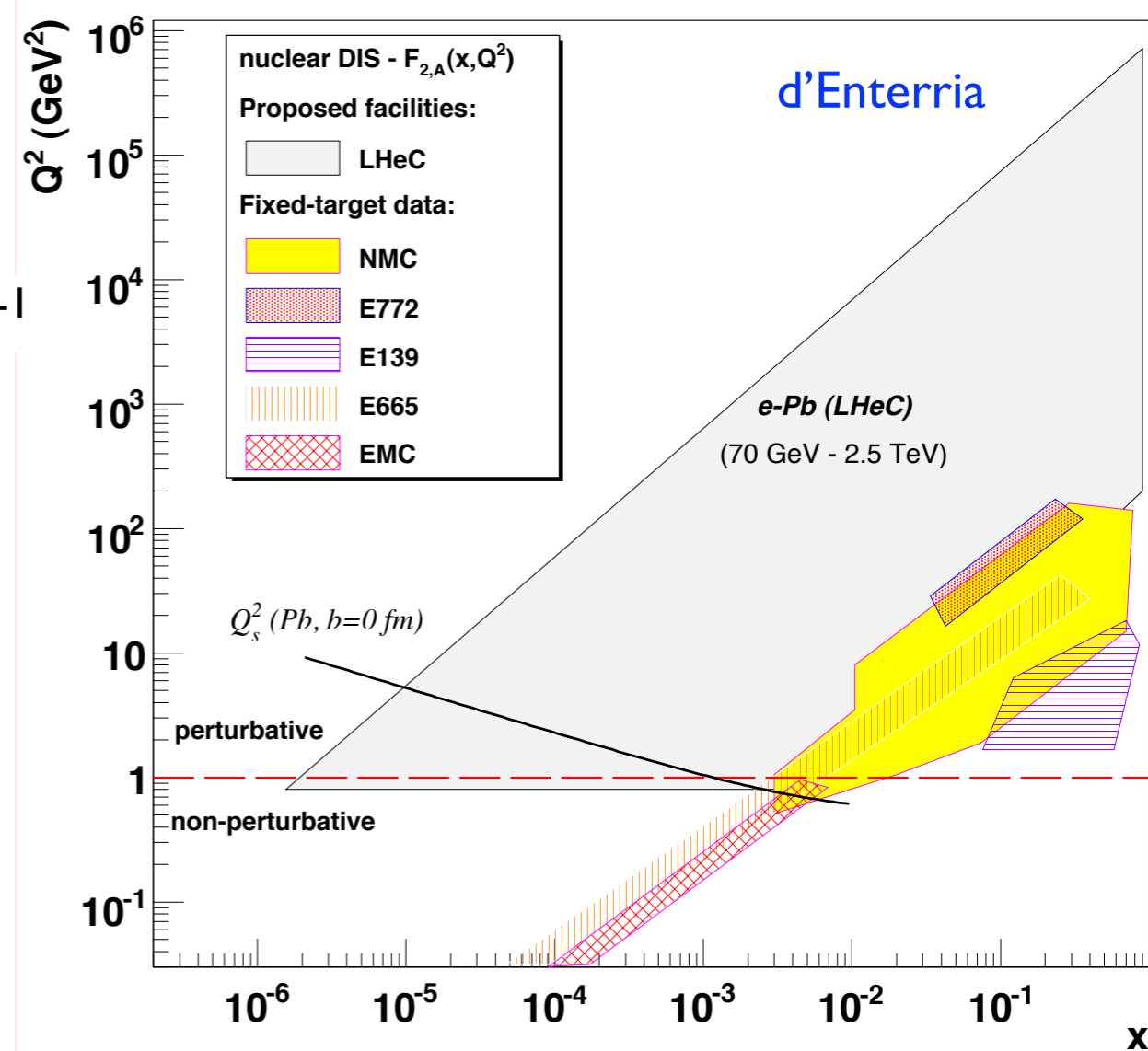
Physics in ep/eA

Kinematics & Motivation (140 GeV x 7 TeV)
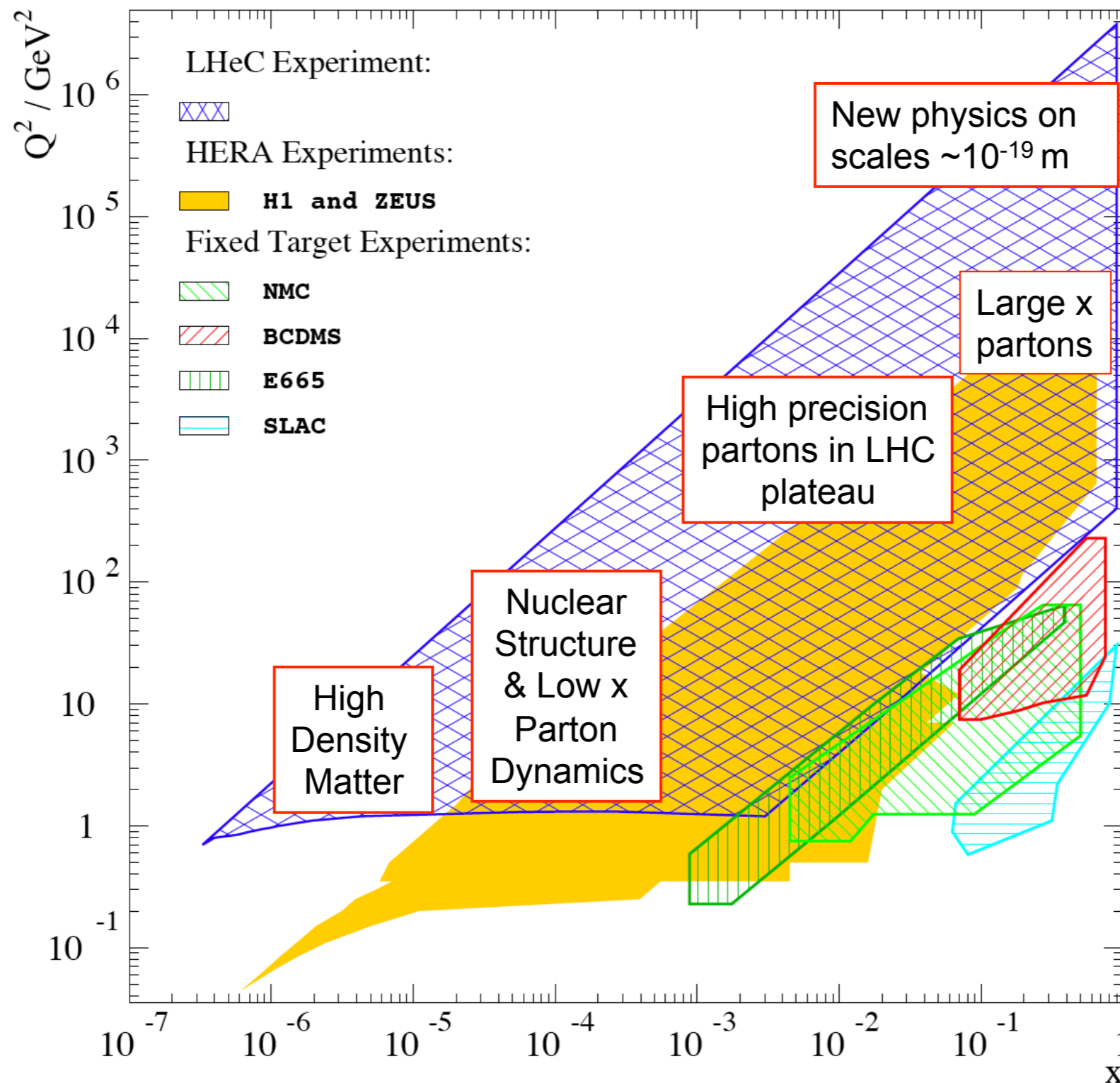
$\sqrt{s}$ = 2 TeV

- High mass (M_{eq}, Q^2) frontier

- EW & Higgs

- Q^2 lever-arm at moderate & high x → PDFs

- Low x frontier → novel QCD ...

$x \geq 5.10^{-7}$ at $Q^2 \leq 1\,\mathrm{GeV}^2$

EIC: eRHIC and ELIC

ep mode:

$$E_e = 5 - 30 \text{ GeV}$$

$$E_p = 50 - 250(325) \text{ GeV}$$

$$\sqrt{s} = 30 - 200 \text{ GeV}$$

$$L \sim 10^{33-34} \text{ cm}^{-2}\text{s}^{-1}$$

Beam polarization: 70% for $p, D, {}^3He$

eA mode:

$$p \to U$$

$$E_A = 20 - 100 \text{ GeV/N}$$

$$\sqrt{s} = 12 - 63 \text{ GeV}$$

$$L_A/N \sim 10^{33} \text{ cm}^{-2}\text{s}^{-1}$$
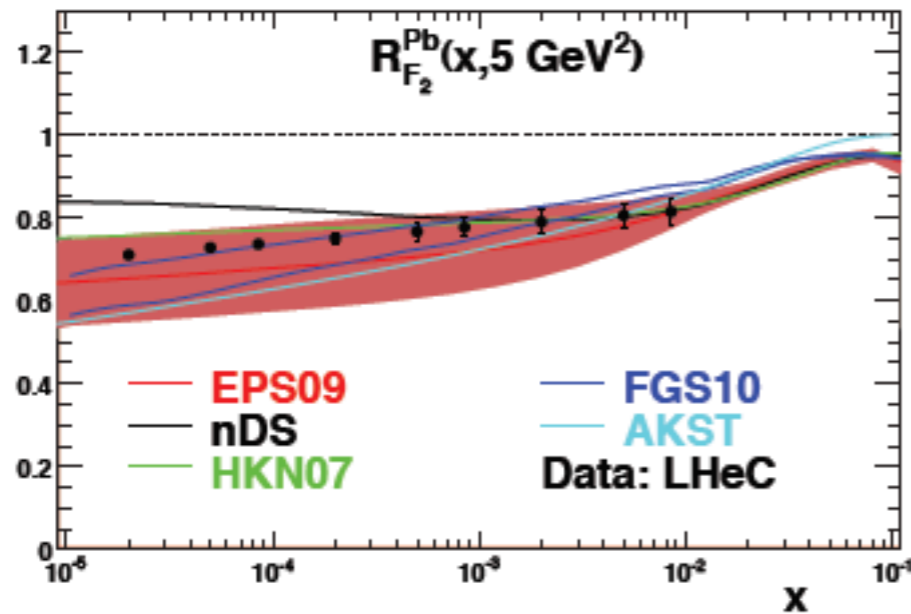
Q^2 (GeV^2)

Abhay Deshpande at RBRC

- HERA
- Fixed target μ-DIS
- Fixed target e-DIS
- EIC

x
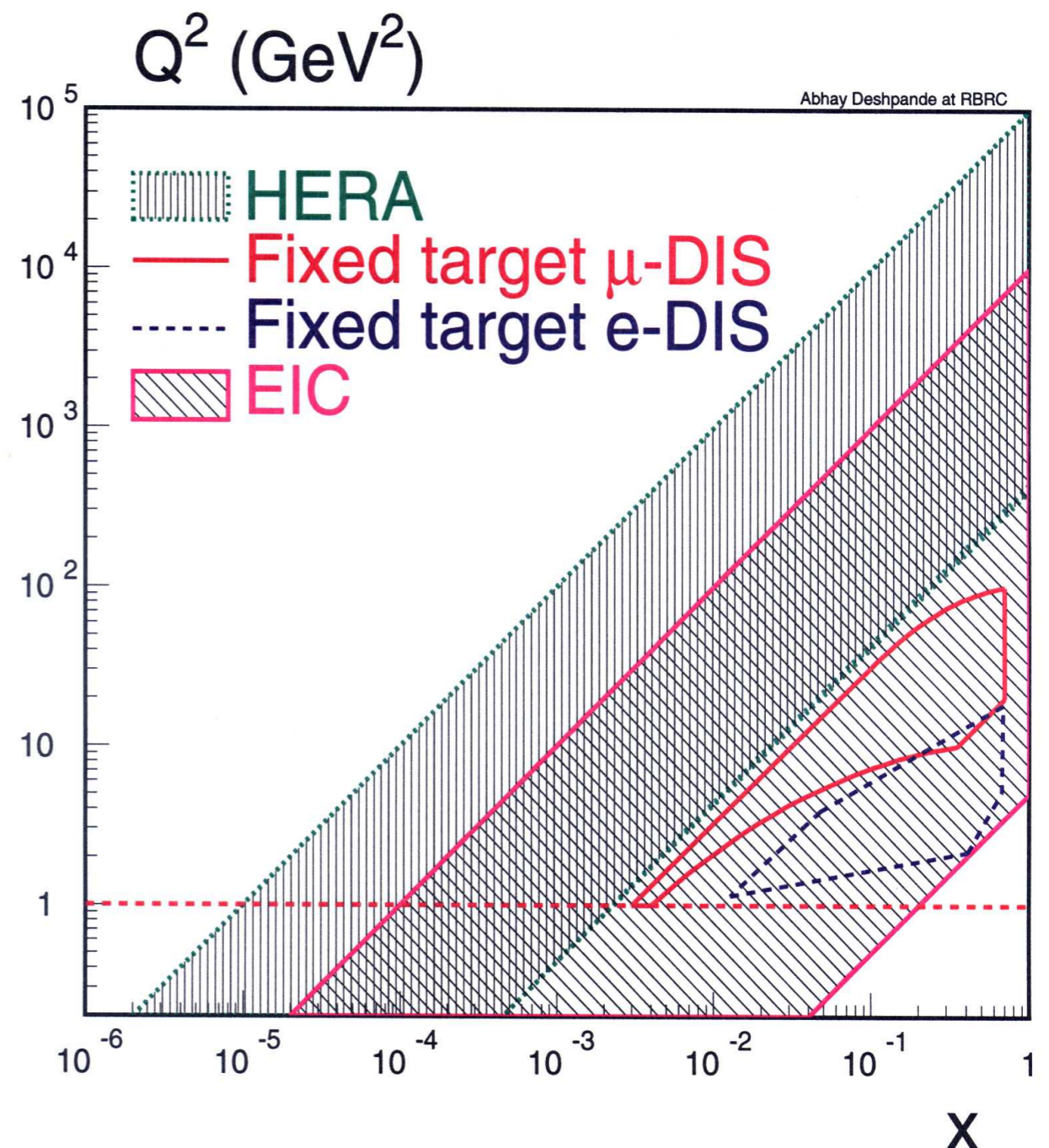
Nuclear structure functions

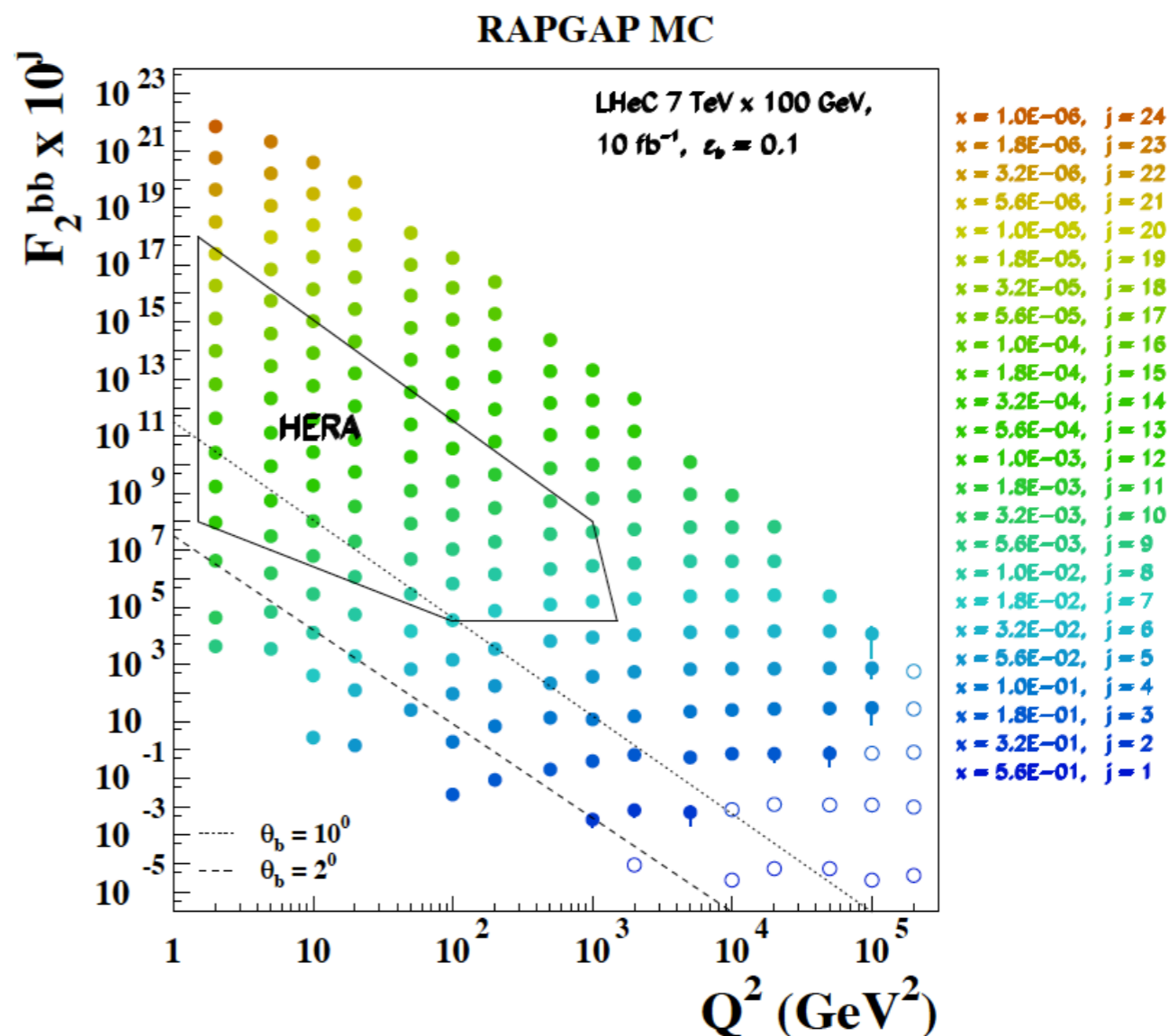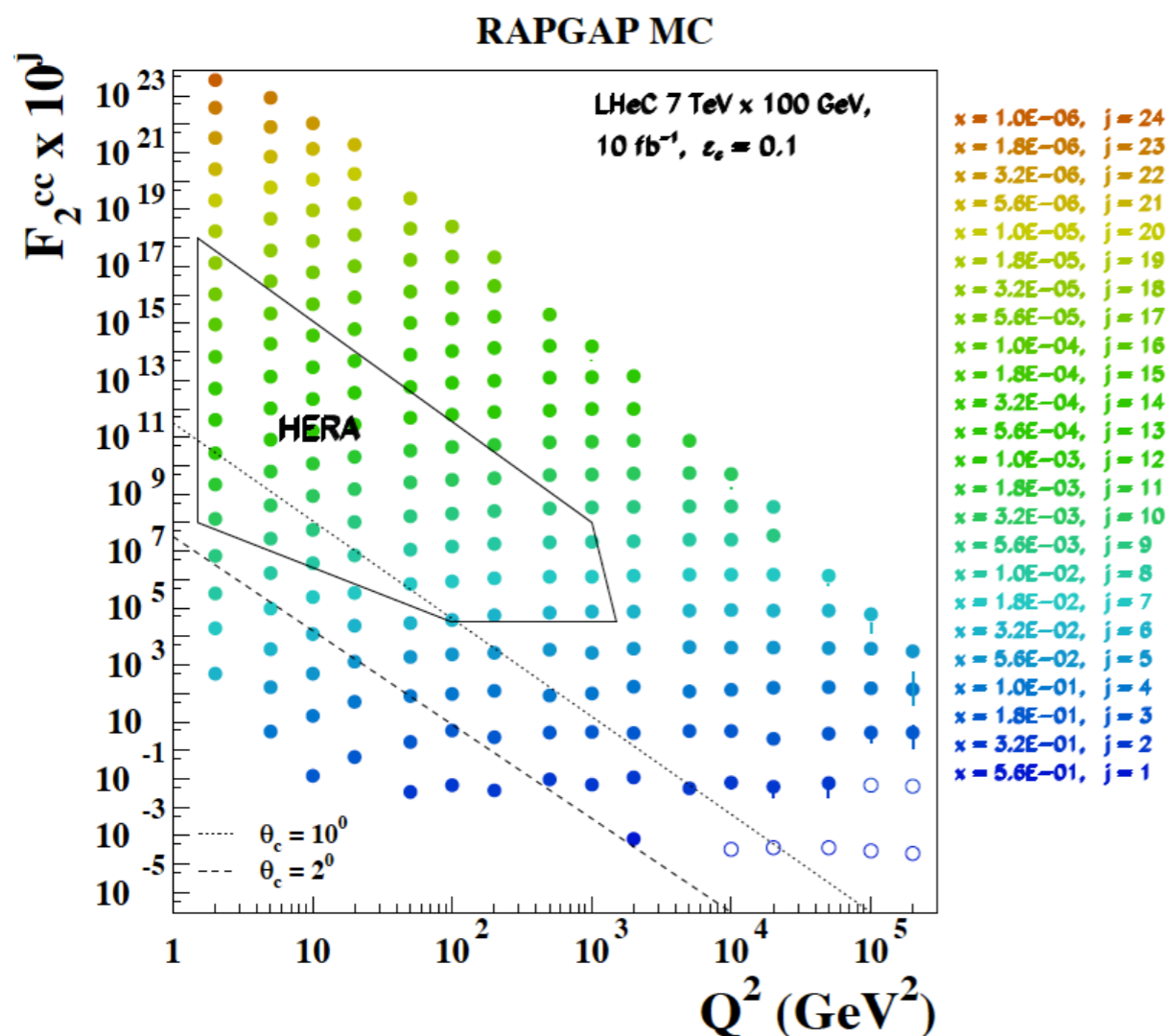- Excellent precision on F_2
- Heavy flavor components
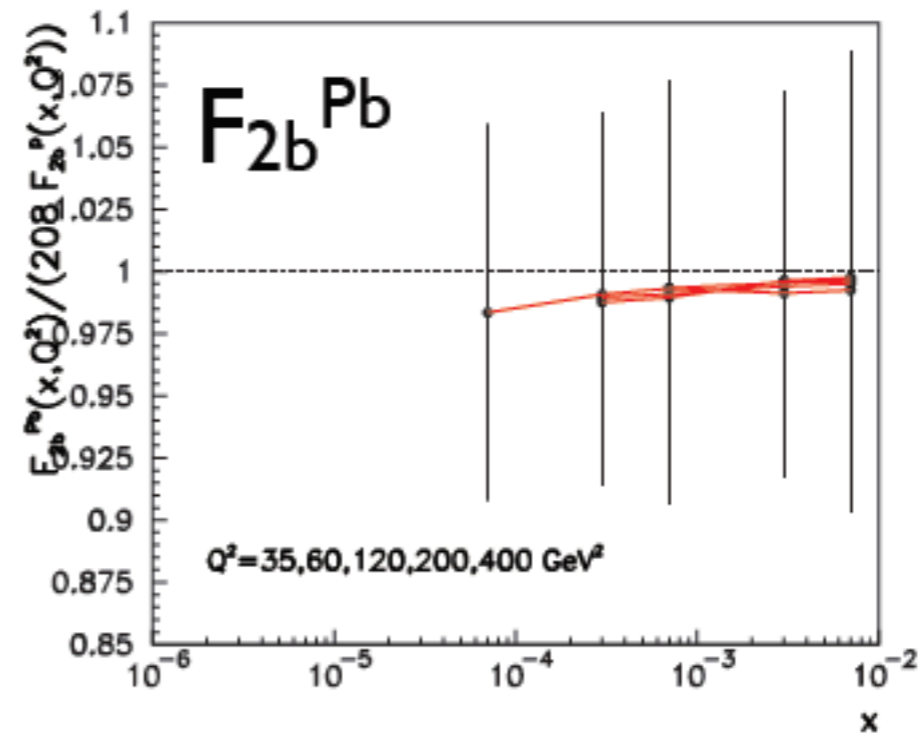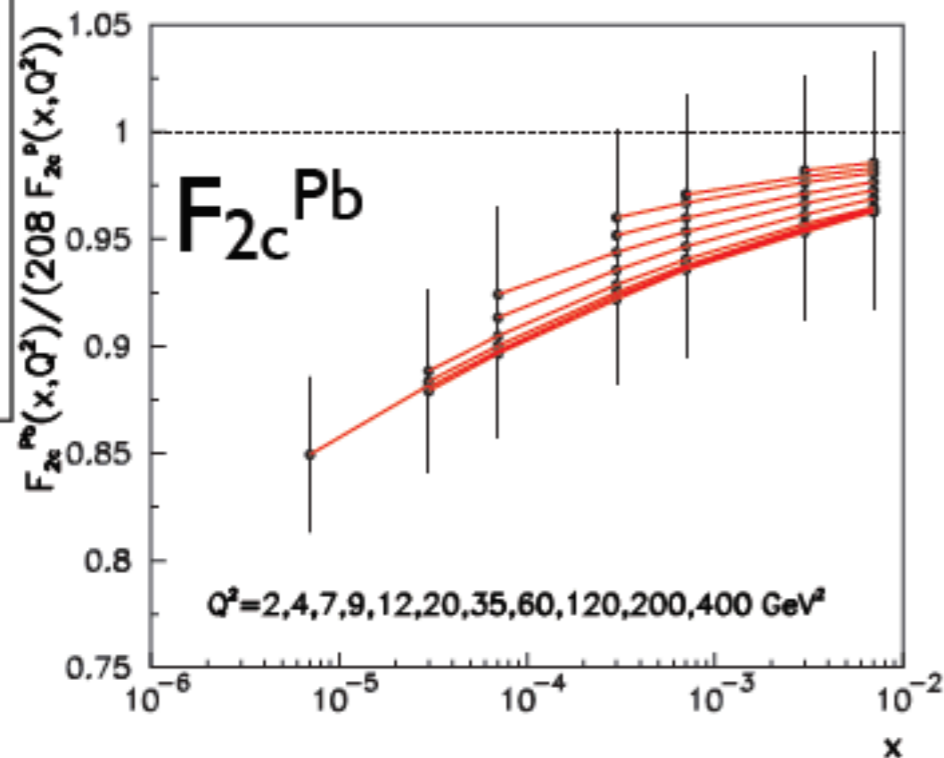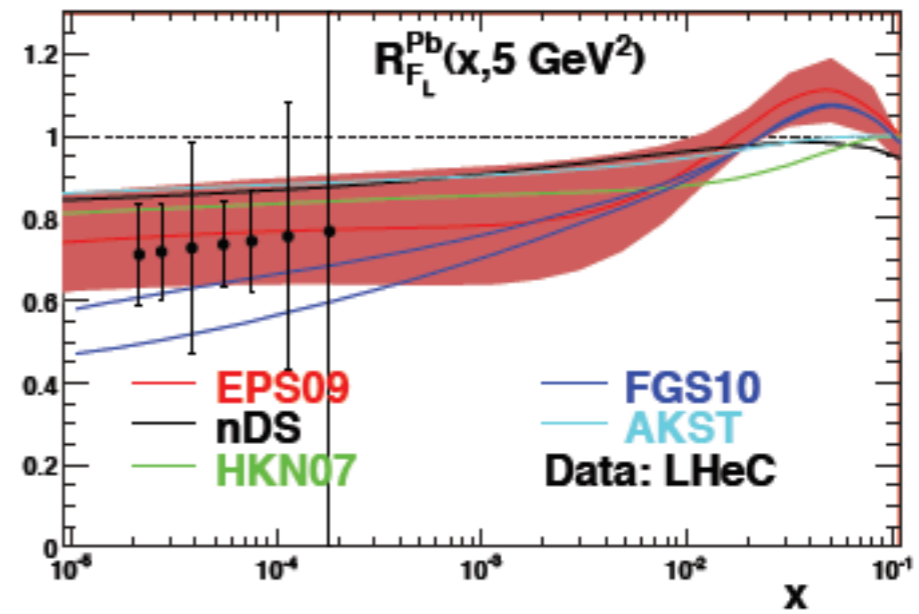
Note on heavy flavor in ep

Simulations with RAPGAP MC 3.1

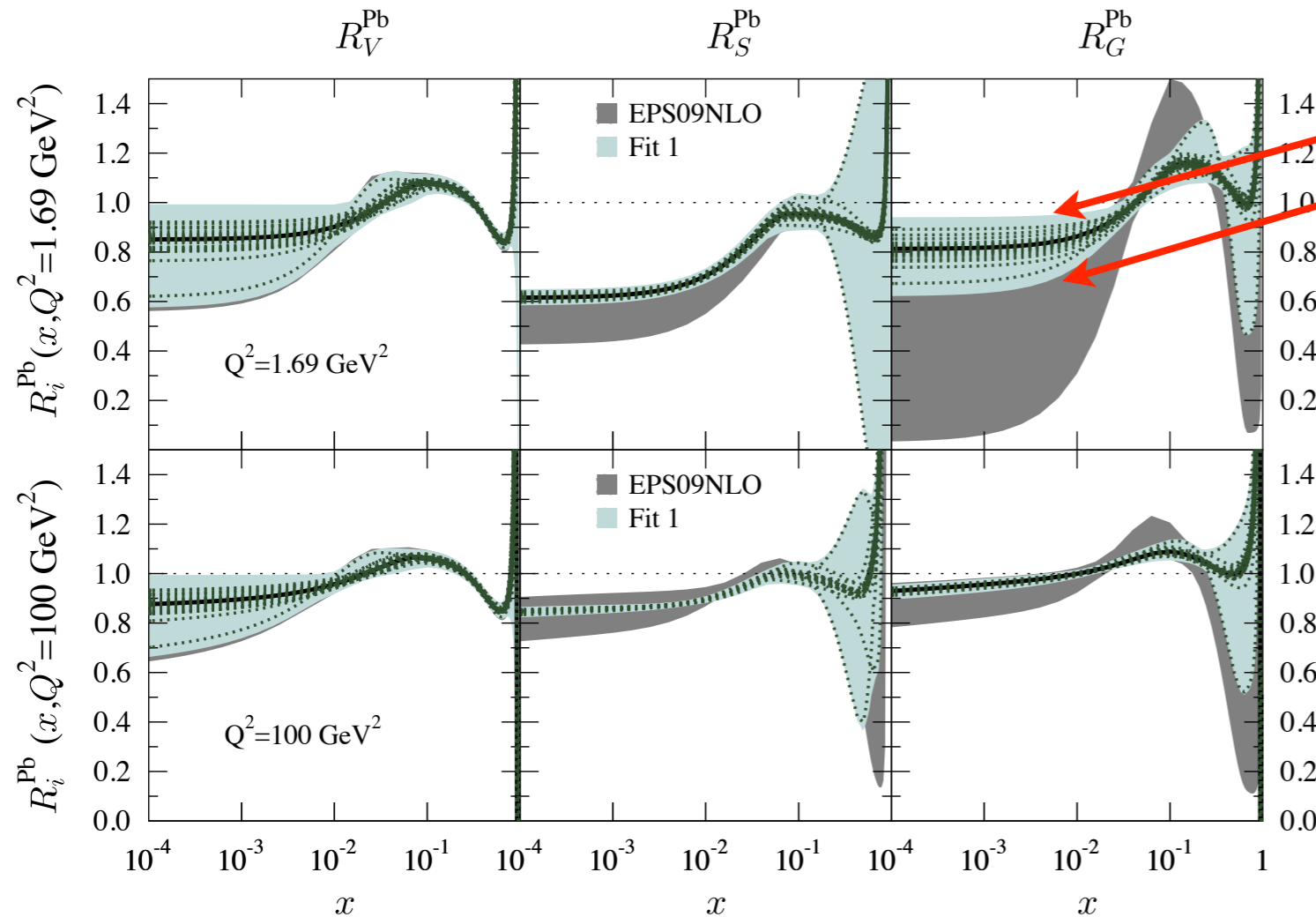Impressive extension of the phase space.
Both small and large x.

Crucial as a benchmark for the heavy flavor production in nuclei. Can test thoroughly the nuclear effects of in heavy quark production.

Impact of LHeC on nuclear parton distributions

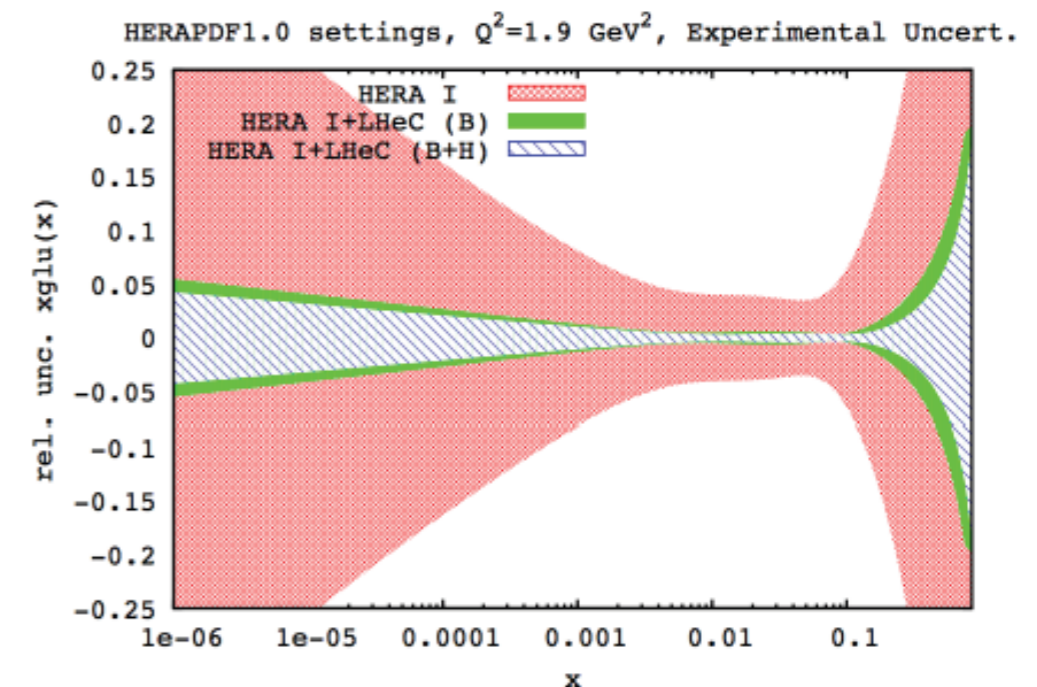Global NLO fit with the LHeC pseudodata included

R_V^{Pb} R_S^{Pb} R_G^{Pb}

Much smaller uncertainties.

Strong constraint on the low x gluons and sea quarks after the inclusion of the LHeC pseudodata in the fits.

Gluon in the proton

Constraining gluon/sea densities simultaneously for proton and Pb.

Longitudinal structure function in ep/eA

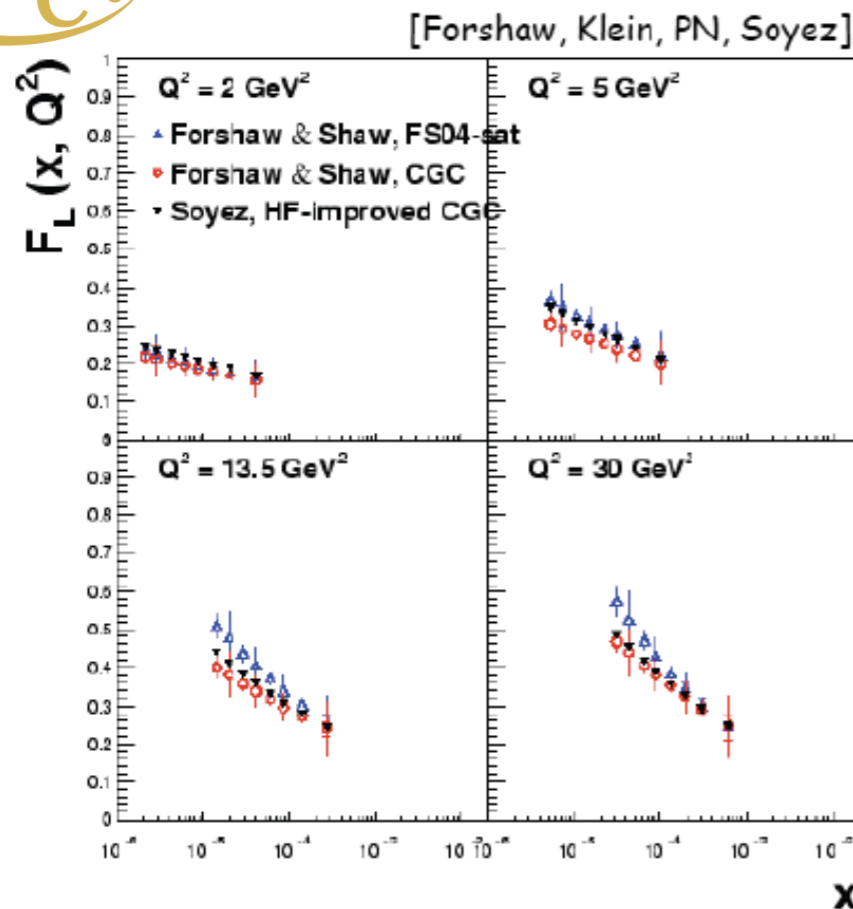It is known from theory that F_L is sensitive to the gluon distribution.

Vanishes in naiive parton model (when transverse momenta limited).

Dominant contribution: $g \rightarrow q\bar{q}$

But.... it is also known experimentally that it is challenging measurement.
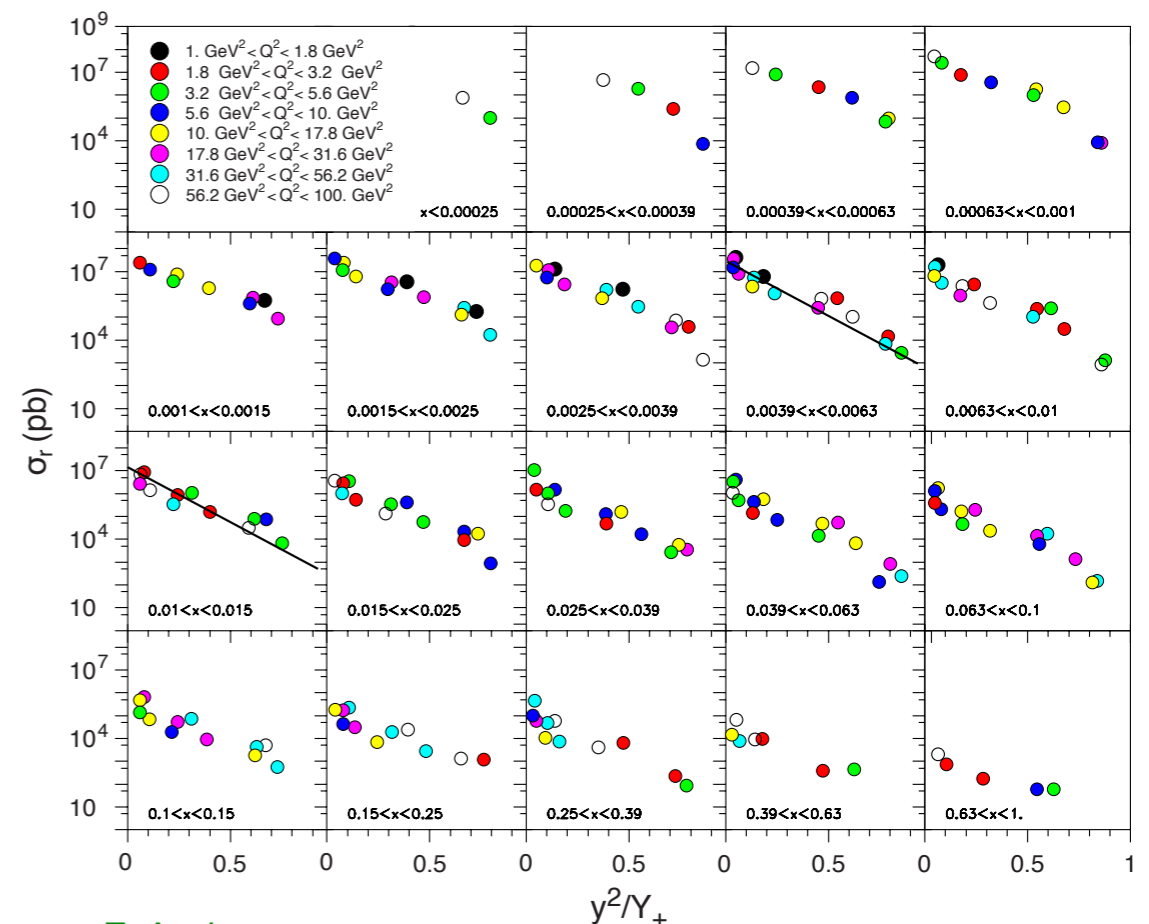Need y dependence, varying energies.

$$\sigma_r^{NC} = \frac{Q^4 x}{2\pi\alpha^2 Y_+}\frac{d^2\sigma^{NC}}{dx dQ^2} = F_2\left[1 - \frac{y^2}{Y_+}\frac{F_L}{F_2}\right], \qquad Y_+ = 1 + (1-y)^2$$

Feasibility study: $\sigma_r = F_2(x,Q^2) - y^2/Y_+ \cdot F_L(x,Q^2)$

$Y_+ = 1 + (1-y)^2$

[Forshaw, Klein, PN, Soyez]

EIC

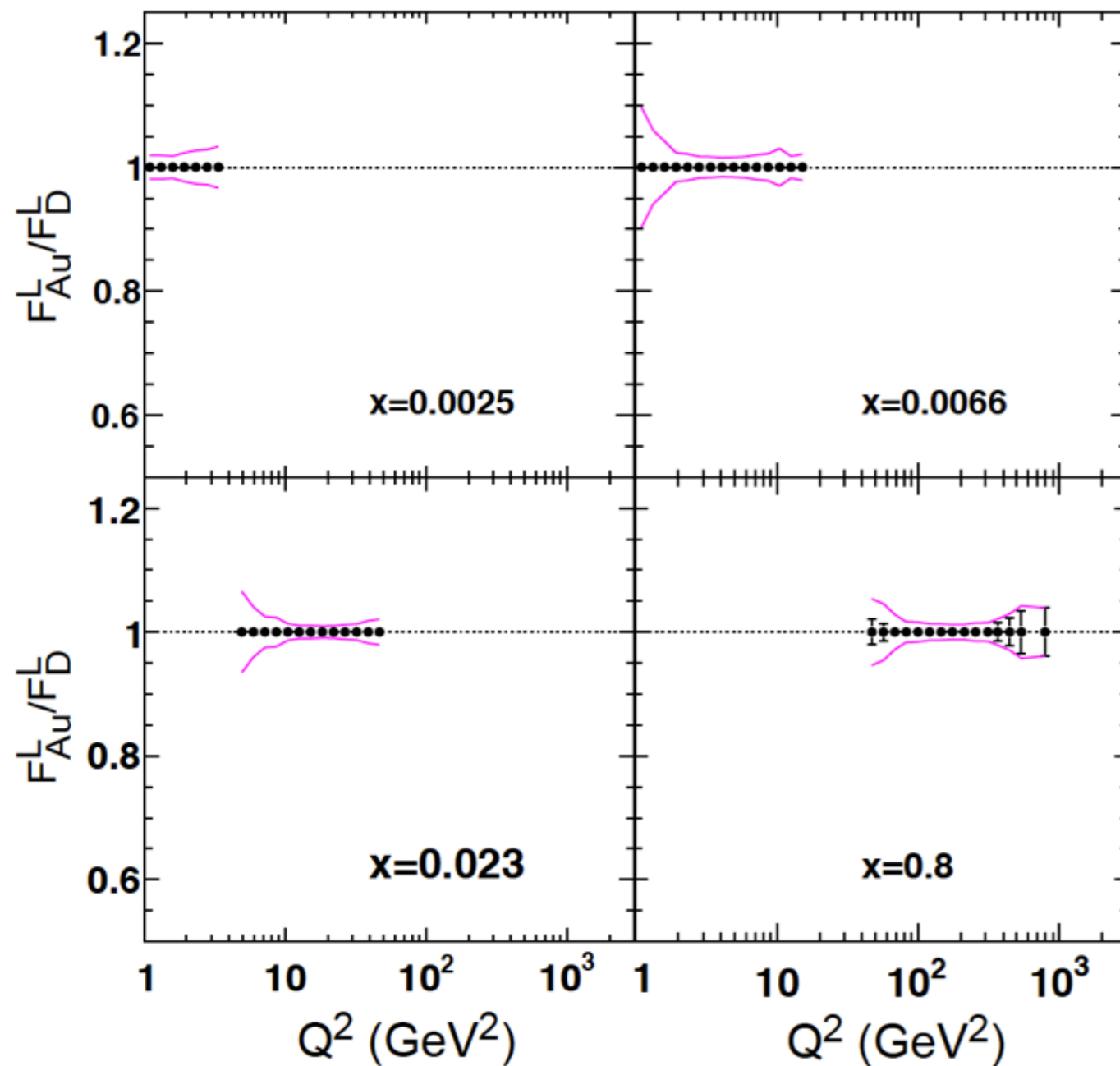Precision typically limited to 5%

Nuclear FL

EIC

$$E_e = 4 \text{ GeV}$$
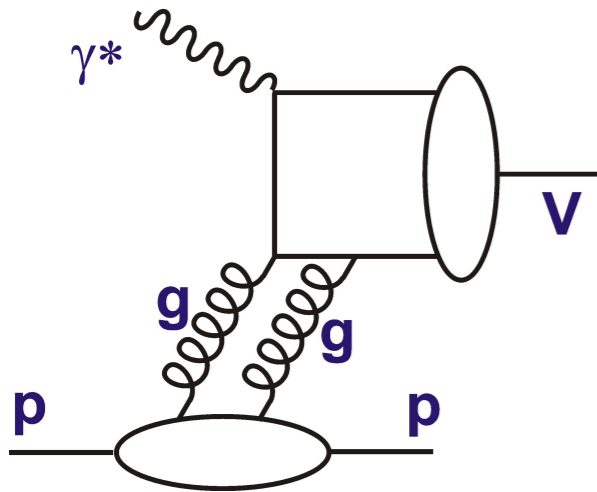
$$E_p = 50, 70, 100, 250 \text{ GeV}$$

Magenta curves show statistical and systematic (1% in normalization) added in quadrature
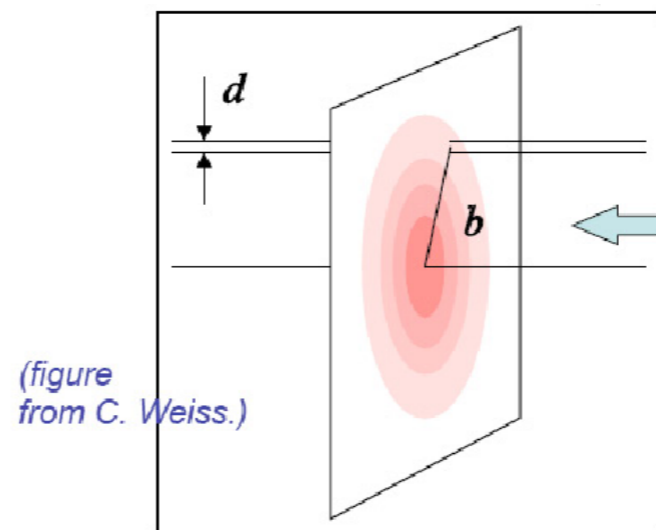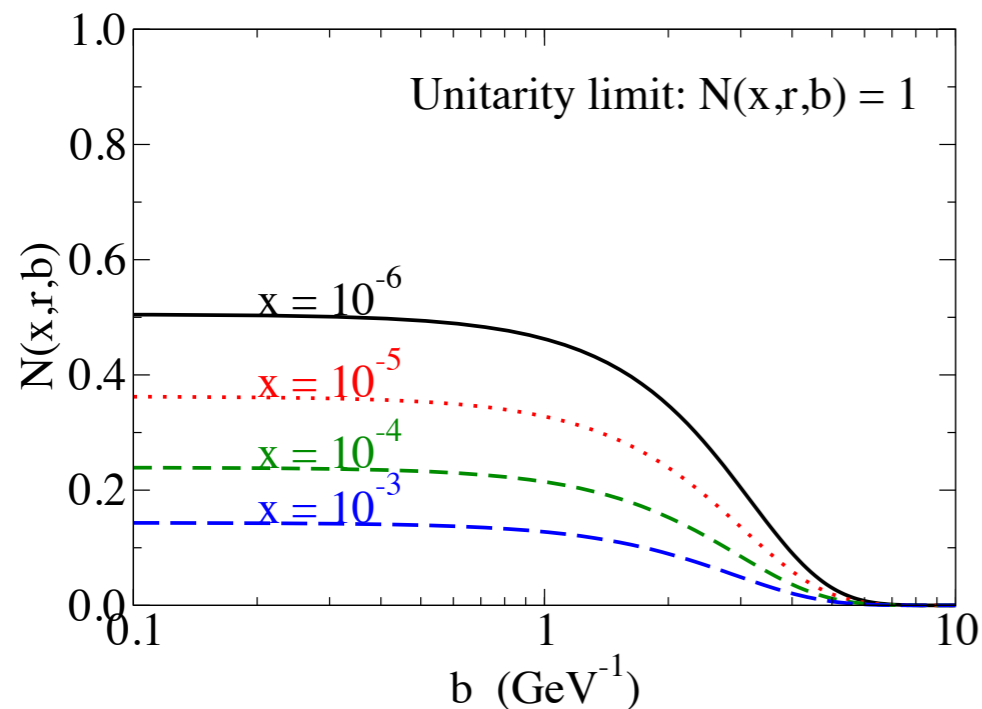
Measurement dominated by the systematic uncertainties.

Issue of e+A radiative corrections...Work in progress

Ullrich DIS2011

Exclusive diffraction

- Exclusive diffractive production of VM is an excellent process for extracting the dipole amplitude

- Suitable process for estimating the 'blackness' of the interaction.

- t-dependence provides an information about the impact parameter profile of the amplitude.

(W)

"b-Sat" dipole scattering amplitude with $r = 1 \, GeV^{-1}$

Unitarity limit: $N(x,r,b) = 1$

$x = 10^{-6}$
$x = 10^{-5}$
$x = 10^{-4}$
$x = 10^{-3}$

$N(x,r,b)$ axis, $b \, (GeV^{-1})$ axis

- b-Sat (eik.)
- b-Sat (1-IP)

$t \, (GeV^2)$

$W = 300 \, GeV$

d Im A($\gamma\, p \to J/\psi\, p$) / db (GeV^{-1}), $b \, (GeV^{-1})$
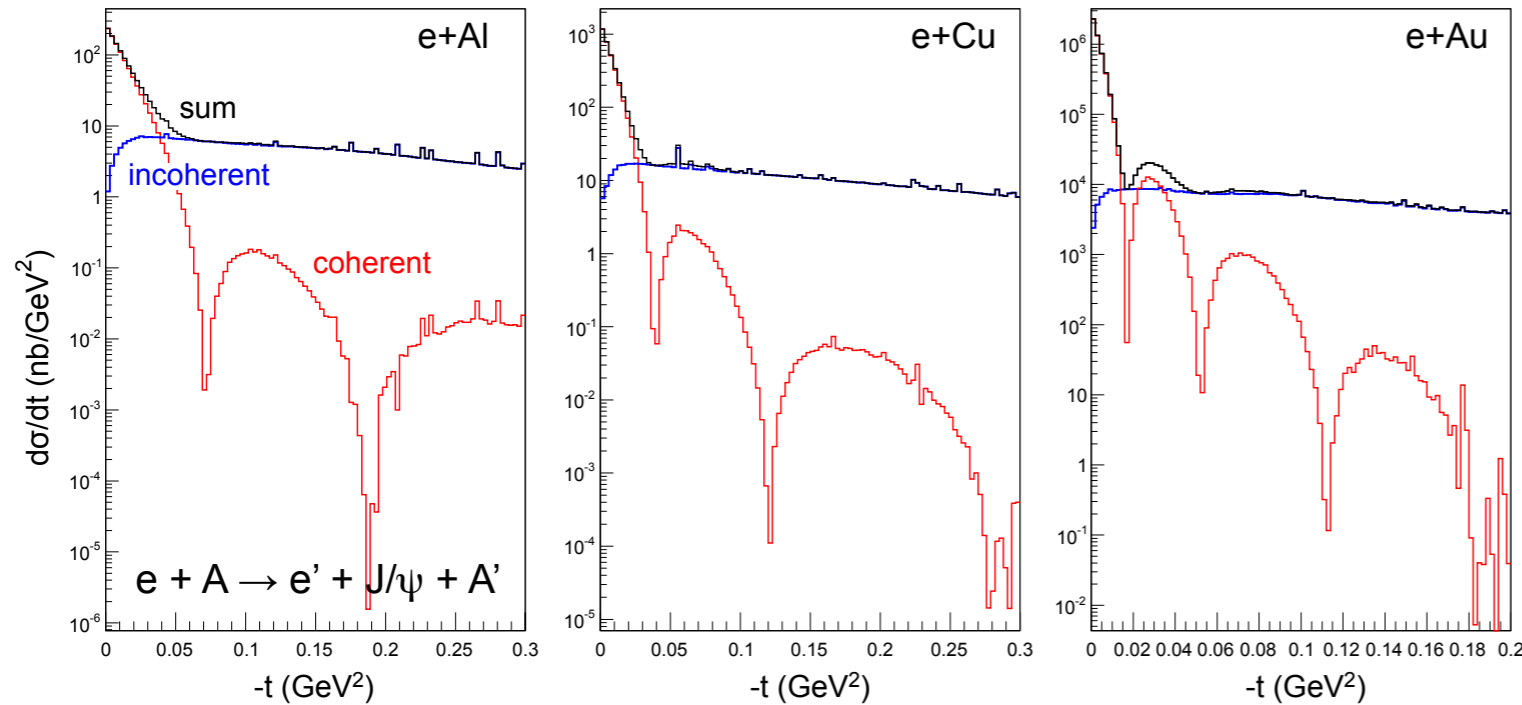
Central black region growing with decrease of x.

Watt

Large momentum transfer t probes small impact parameter where the density of interaction region is most dense.
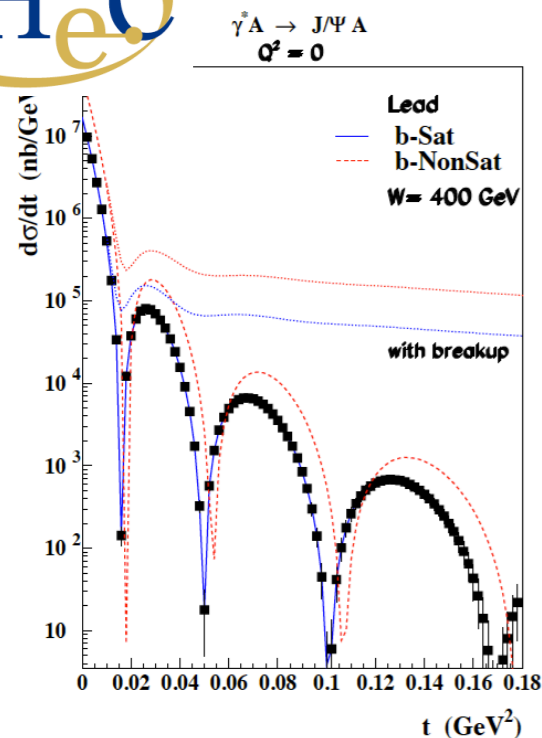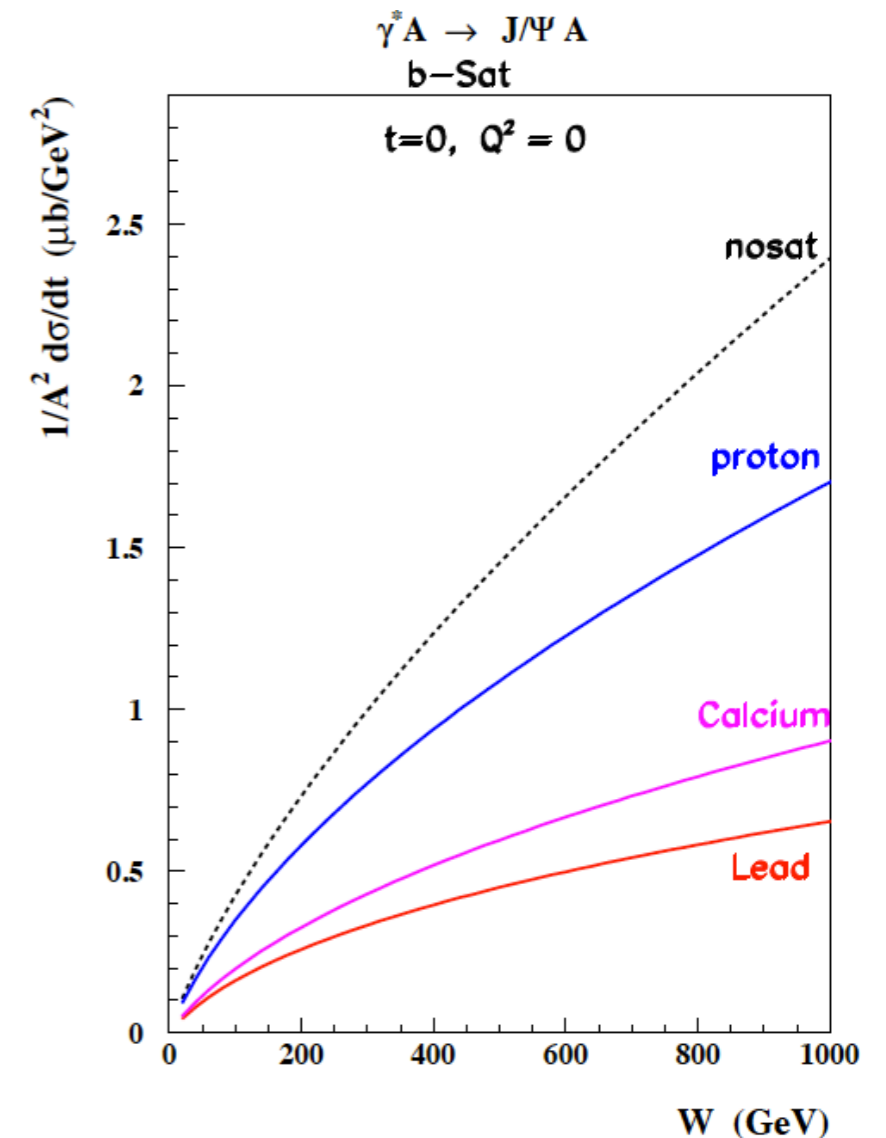
Exclusive diffraction: nuclear case

Possibility of using the same principle to learn about the gluon distribution in the nucleus.
Possible nuclear resonances at small t?

EIC

- Diffractive cross-section $\sigma_{diff}/\sigma_{tot}$ in e+A predicted to be ~25-40%
  - most sensitive to $xG(x,Q^2)$
- Rich physics program on momentum & spatial gluon distribution
- Coherent vs Incoherent: requires detection of breakup with ~ $1\text{-}10^{-4}$ efficiency

t-dependence: characteristic dips. Challenges: need to distinguish between coherent and incoherent diffraction. Need dedicated instrumentation, zero degree calorimeter.

Energy dependence for different targets.

Exclusive diffraction: nuclear case

Exclusive VM production sensitive to the gluon density squared.
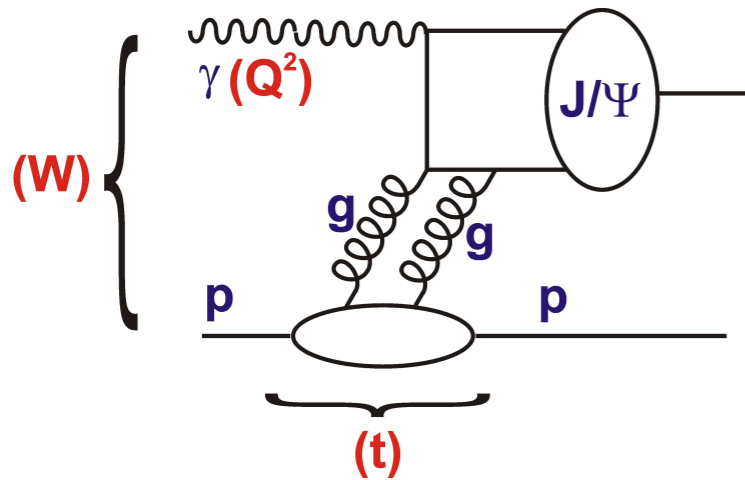
$$\frac{\frac{d\sigma_A}{dt}\big|_{t=0}}{\frac{d\sigma_p}{dt}\big|_{t=0}} \sim \frac{xg_A(x, M^2_{J/\Psi})^2}{xg(x, M^2_{J/\Psi})^2}$$
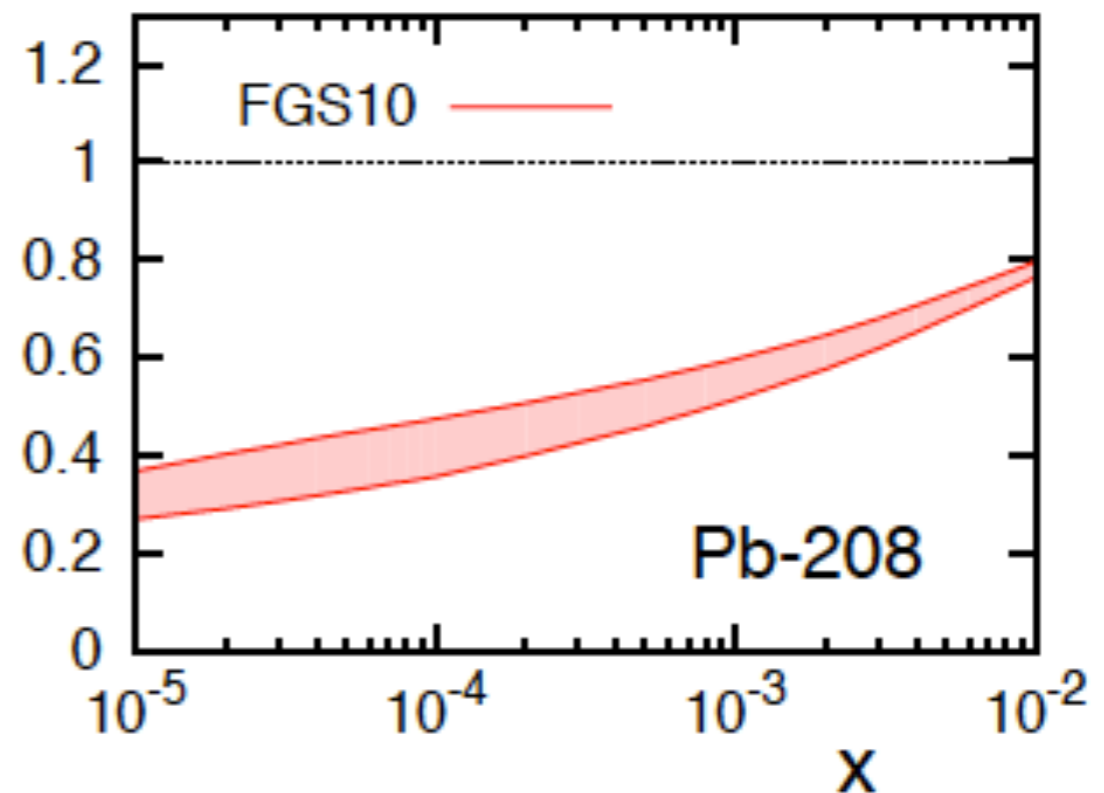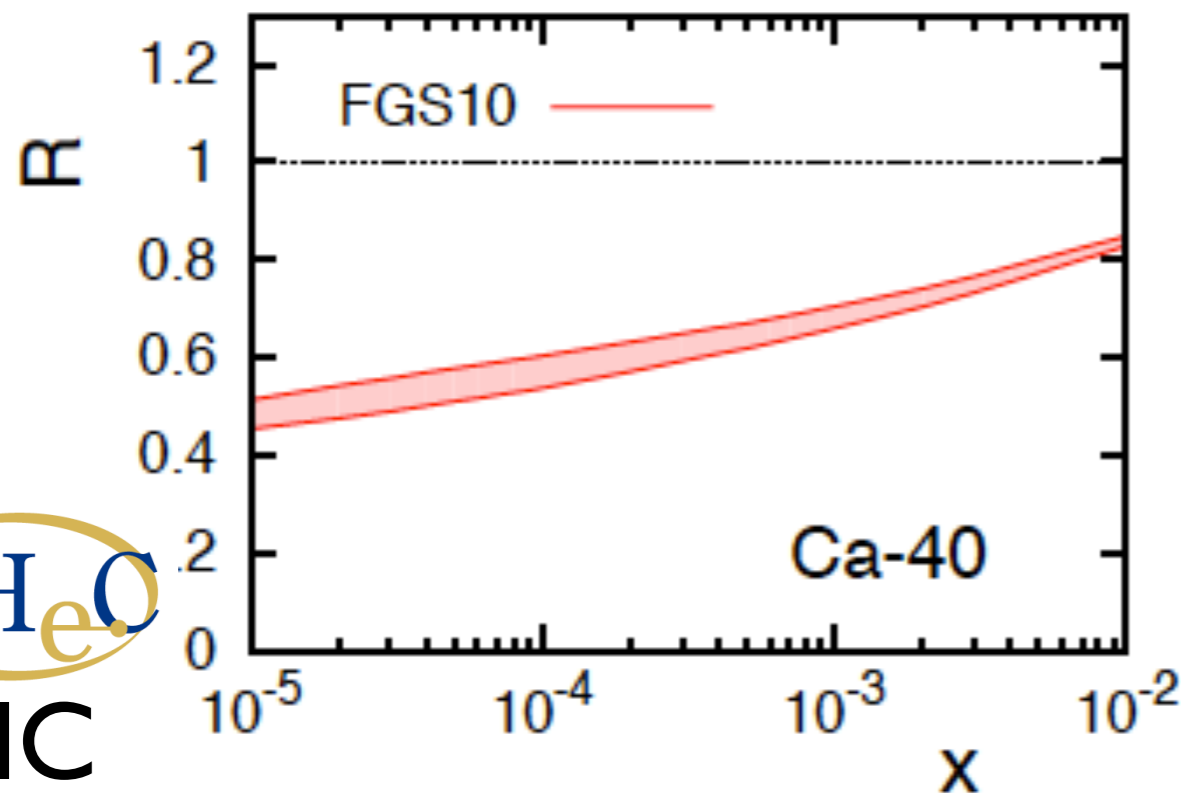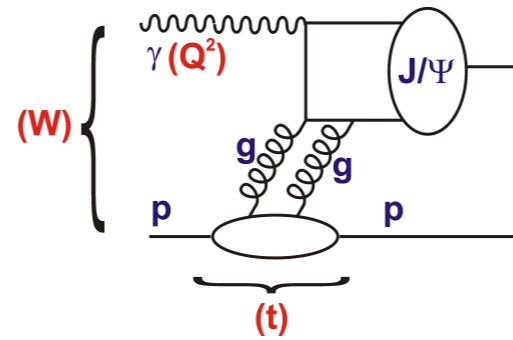

Prediction for the amount of shadowing/saturation in exclusive production

Exclusive diffraction: predictions for ep

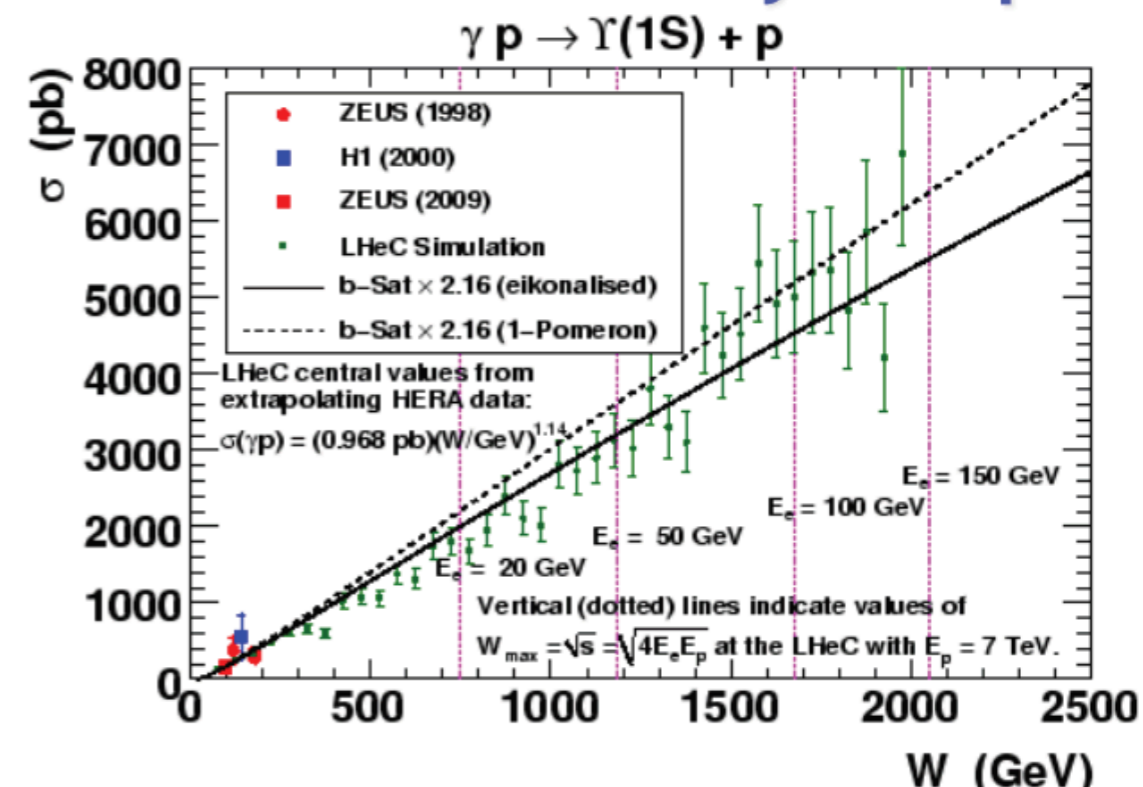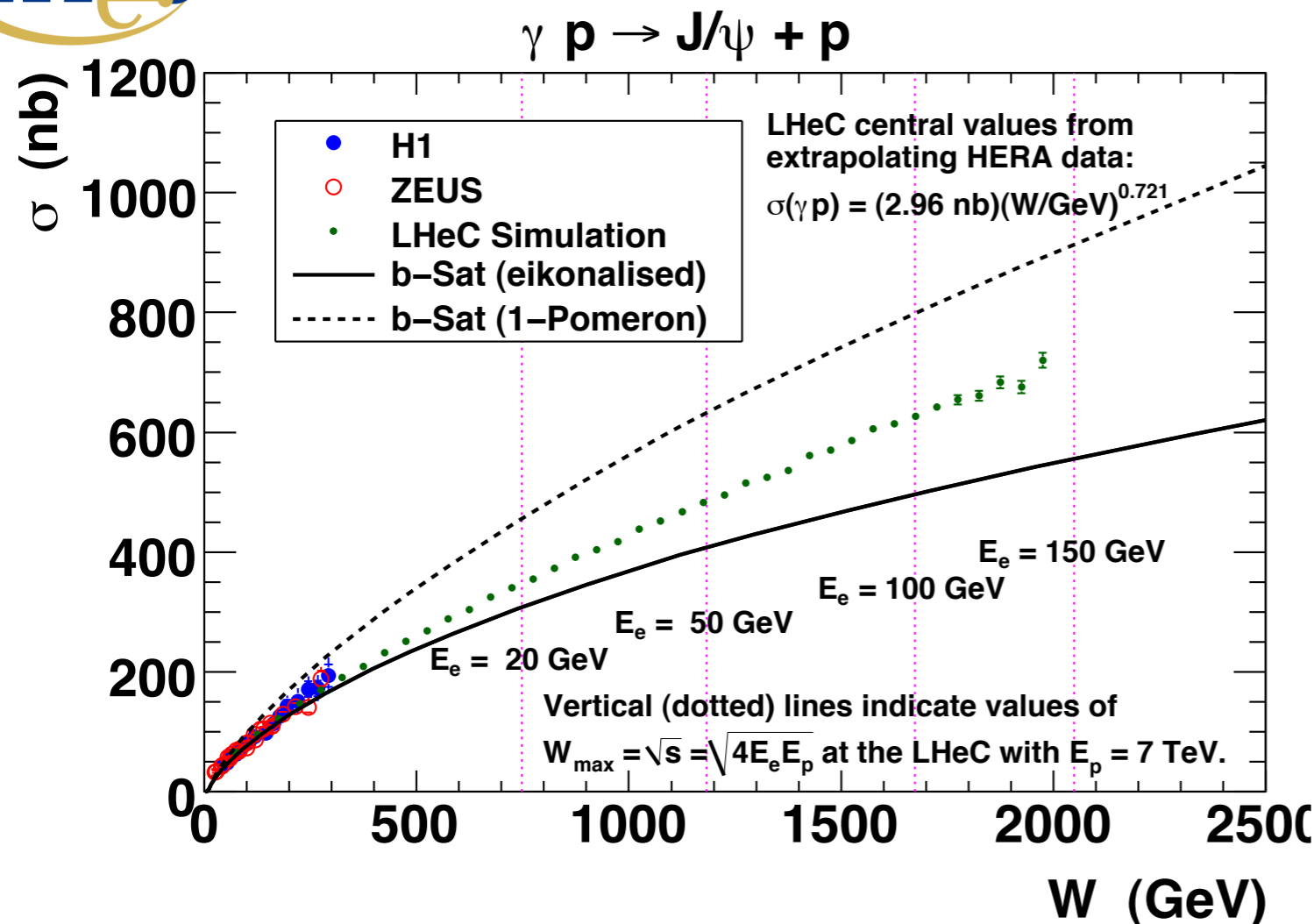$$\sigma^{\gamma p \to J/\Psi + p}(W)$$

- b-Sat dipole model (Golec-Biernat, Wuesthoff, Bartels, Motyka, Kowalski, Watt)
  - eikonalised: with saturation
  - 1-Pomeron: no saturation
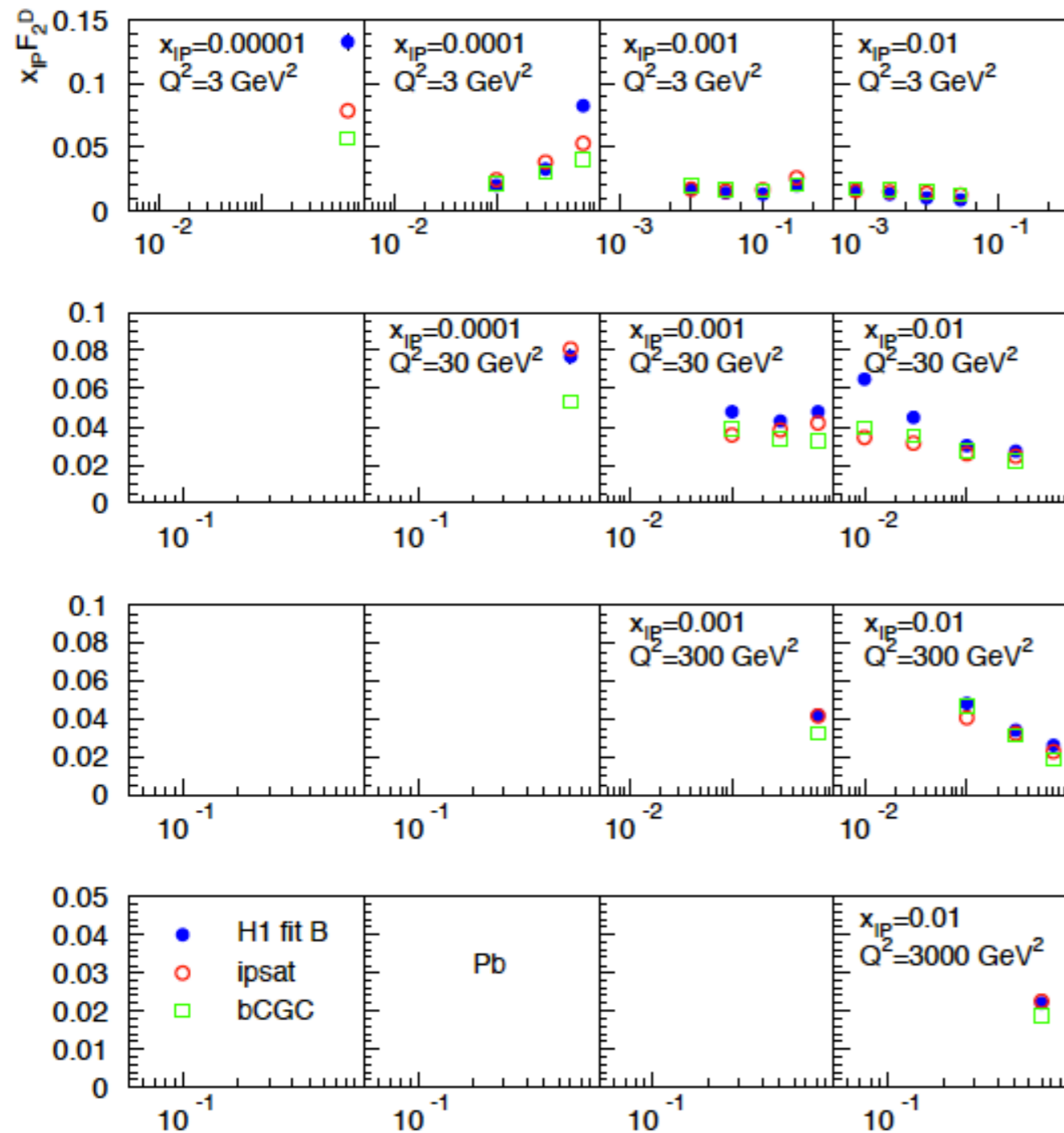
Significant effects even for the t-integrated observable.

Different W behavior depending ether saturation is included or not.

mulated data are from extrapolated fit to HERA data

LHeC can distinguish between the different scenarios.

γ p → J/ψ + p

- H1
- ZEUS
- LHeC Simulation
- b–Sat (eikonalised)
- b–Sat (1–Pomeron)

LHeC central values from extrapolating HERA data:
σ(γp) = (2.96 nb)(W/GeV)^0.721

E_e = 150 GeV
E_e = 100 GeV
E_e = 50 GeV
E_e = 20 GeV

Vertical (dotted) lines indicate values of
$W_{max} = \sqrt{s} = \sqrt{4E_e E_p}$ at the LHeC with E_p = 7 TeV.

γ p → Υ(1S) + p

- ZEUS (1998)
- H1 (2000)
- ZEUS (2009)
- LHeC Simulation
- b–Sat × 2.16 (eikonalised)
- b–Sat × 2.16 (1–Pomeron)

LHeC central values from extrapolating HERA data:
σ(γp) = (0.968 pb)(W/GeV)^1.14

E_e = 150 GeV
E_e = 100 GeV
E_e = 50 GeV
E_e = 20 GeV

Vertical (dotted) lines indicate values of
$W_{max} = \sqrt{s} = \sqrt{4E_e E_p}$ at the LHeC with E_p = 7 TeV.

Inclusive diffraction in eA

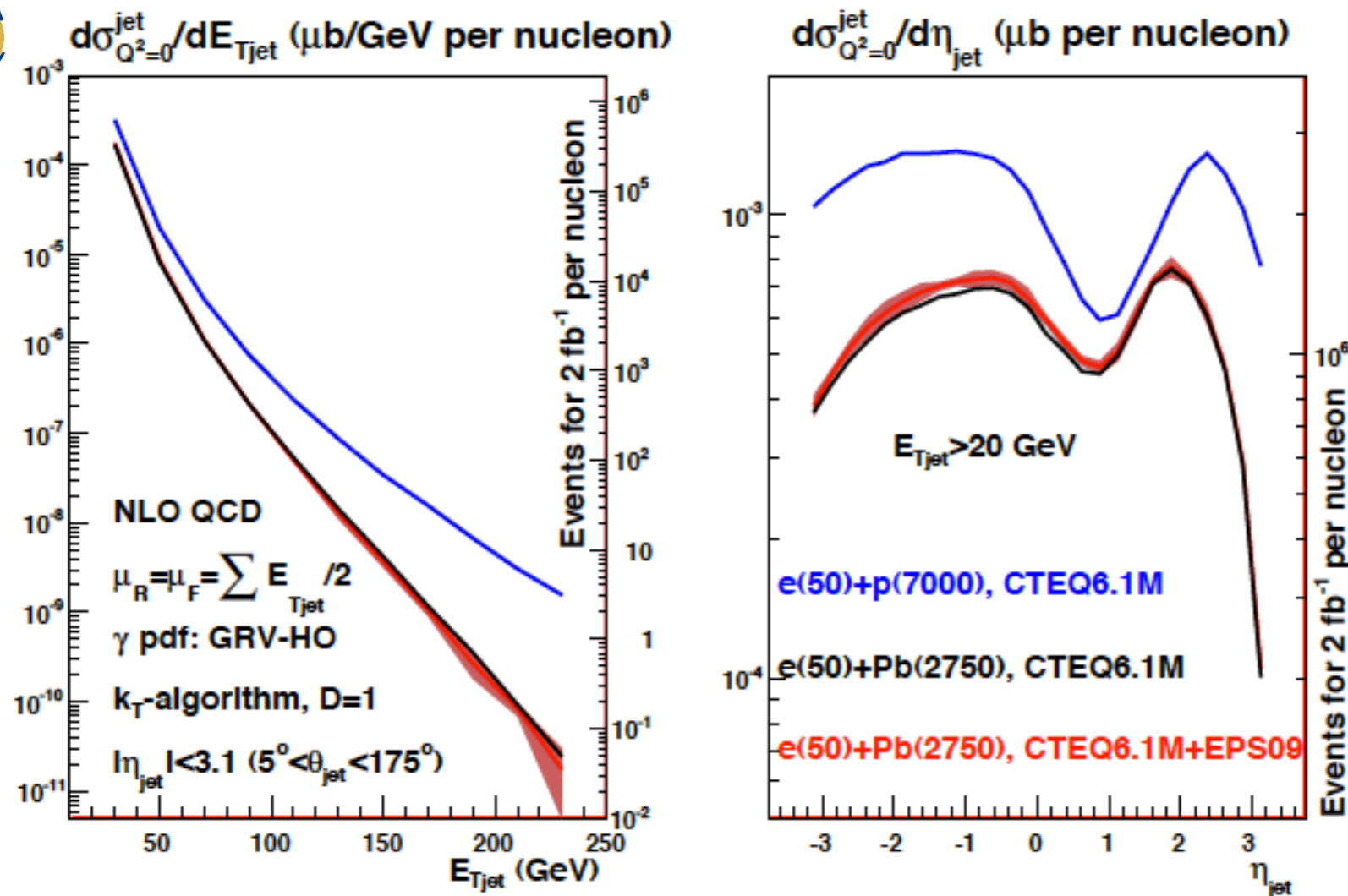## Diffractive structure function for Pb

Diffractive to inclusive ratio for protons and Pb
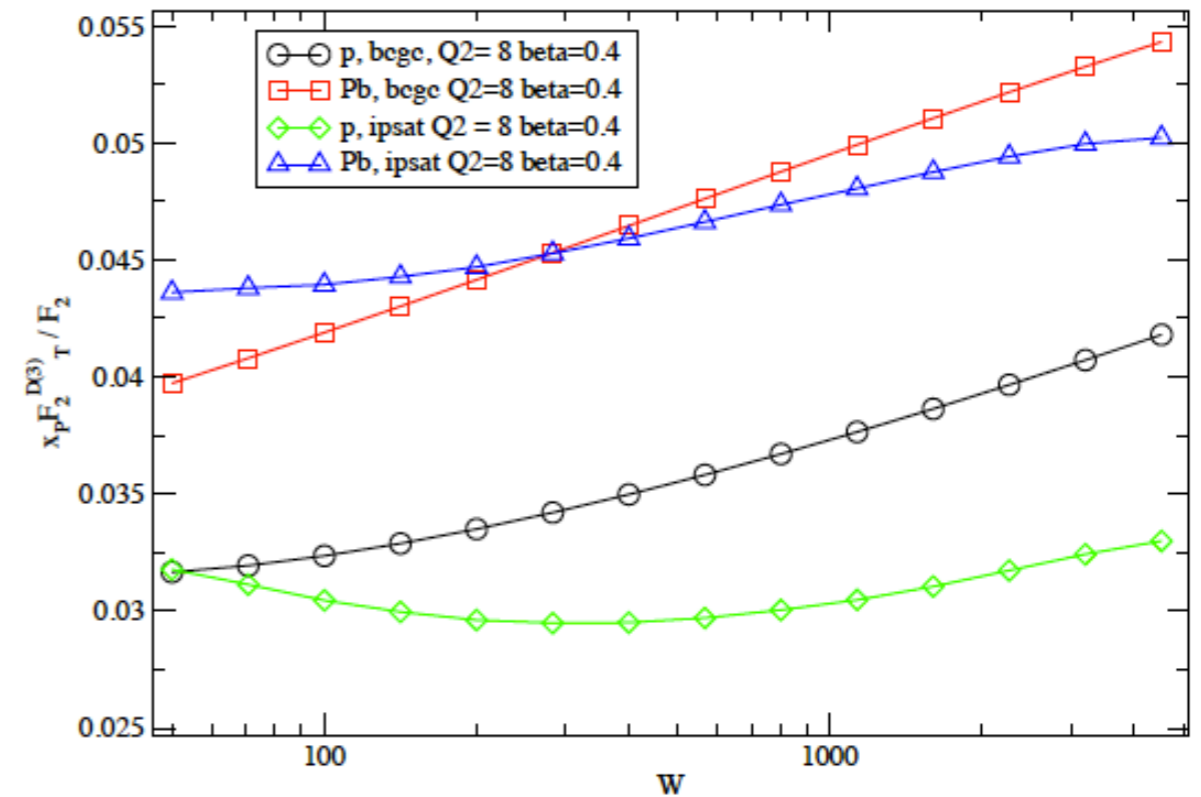
Enhanced diffraction in the nuclear case

Study of diffractive dijets, heavy quarks for the factorization tests

Final states: jet photoproduction

$E_e = 50 \text{ GeV}$

$E_T > 20 \text{ GeV}$

$|\eta_{\text{jet}}| < 3.1$

$L = 2 \text{ fb}^{-1}$

Two-peak structure: direct and resolved.

Need to do: background subtraction, detailed analysis of jet reconstruction, energy calibration.

Hard probe of the nuclear medium.
Information about photon structure.

Summary

- eA(with parallel ep) at high energy essential to untangle the complex nuclear structure at low x and constrain the initial conditions for AA. Also low x ep needed for pp, low x, forward rapidities. Entering new regime of DIS with high parton densities. Precision DIS measurements complementary to pp/pA/AA.

- LHeC program: complete flavor decomposition of pdfs, heavy flavor measurement at high accuracy, precision strong coupling measurements, electroweak couplings, TMD and GPD, high parton density/saturation at low x, nuclear effects, BSM...

- EIC program: nuclear structure at moderately low x by scanning A dependence from light to heavy nuclei, nuclear pdfs, TMD and GPD measurement, spin structure (for p and d), polarized sea and gluons...

- Timeline for LHeC: first version of CDR (almost) complete. Realization in 10 years or so.

- Timeline for EIC: staged approach; construction ELIC in 10 years, eRHIC first stage in about or less than 10 years.

Backup

Predictions for the proton

DGLAP approaches have large uncertainties at low x and even at moderate Q (larger uncertainties as Q is decreased)
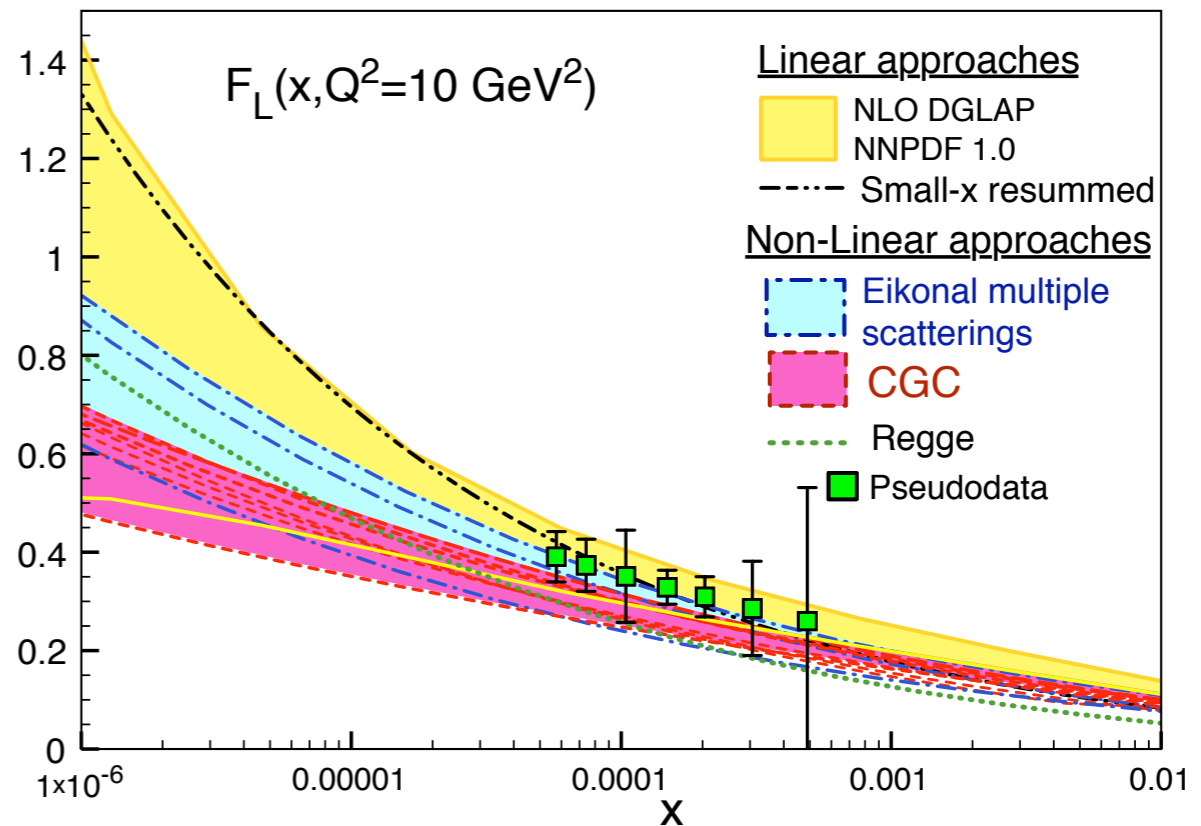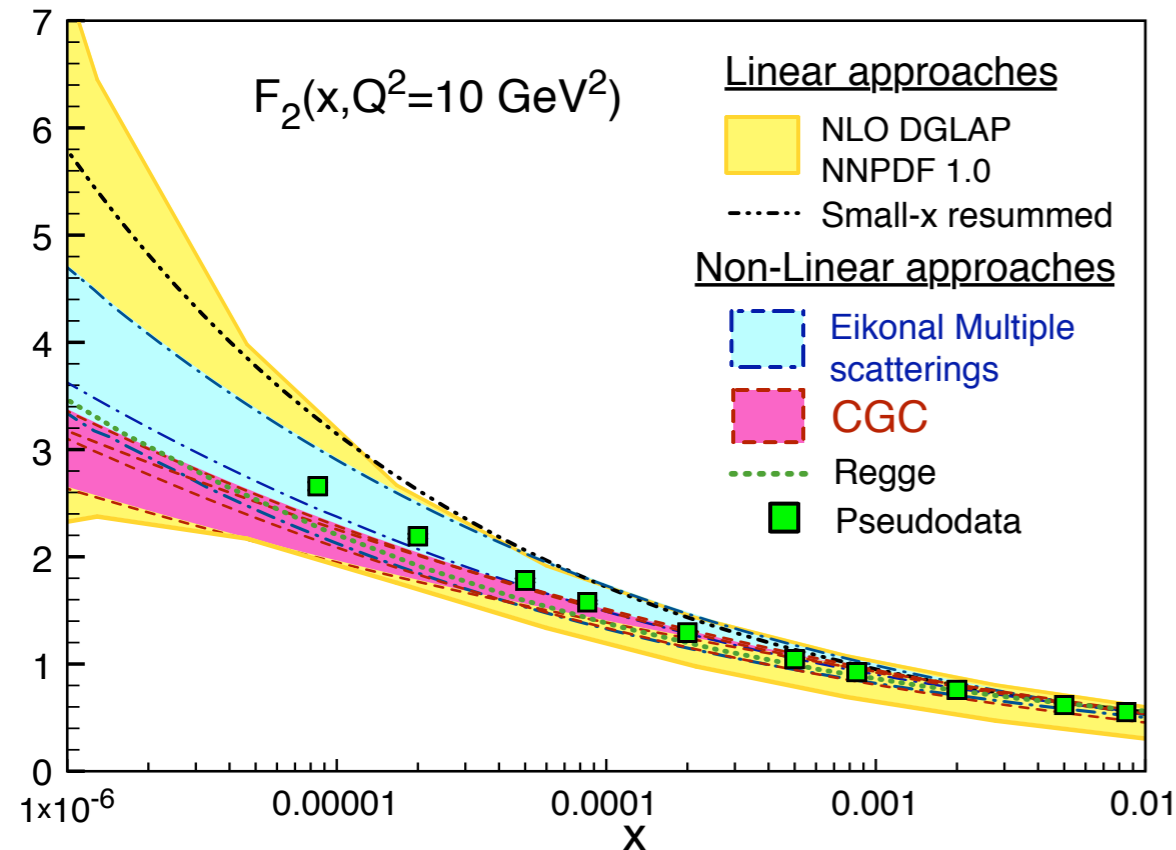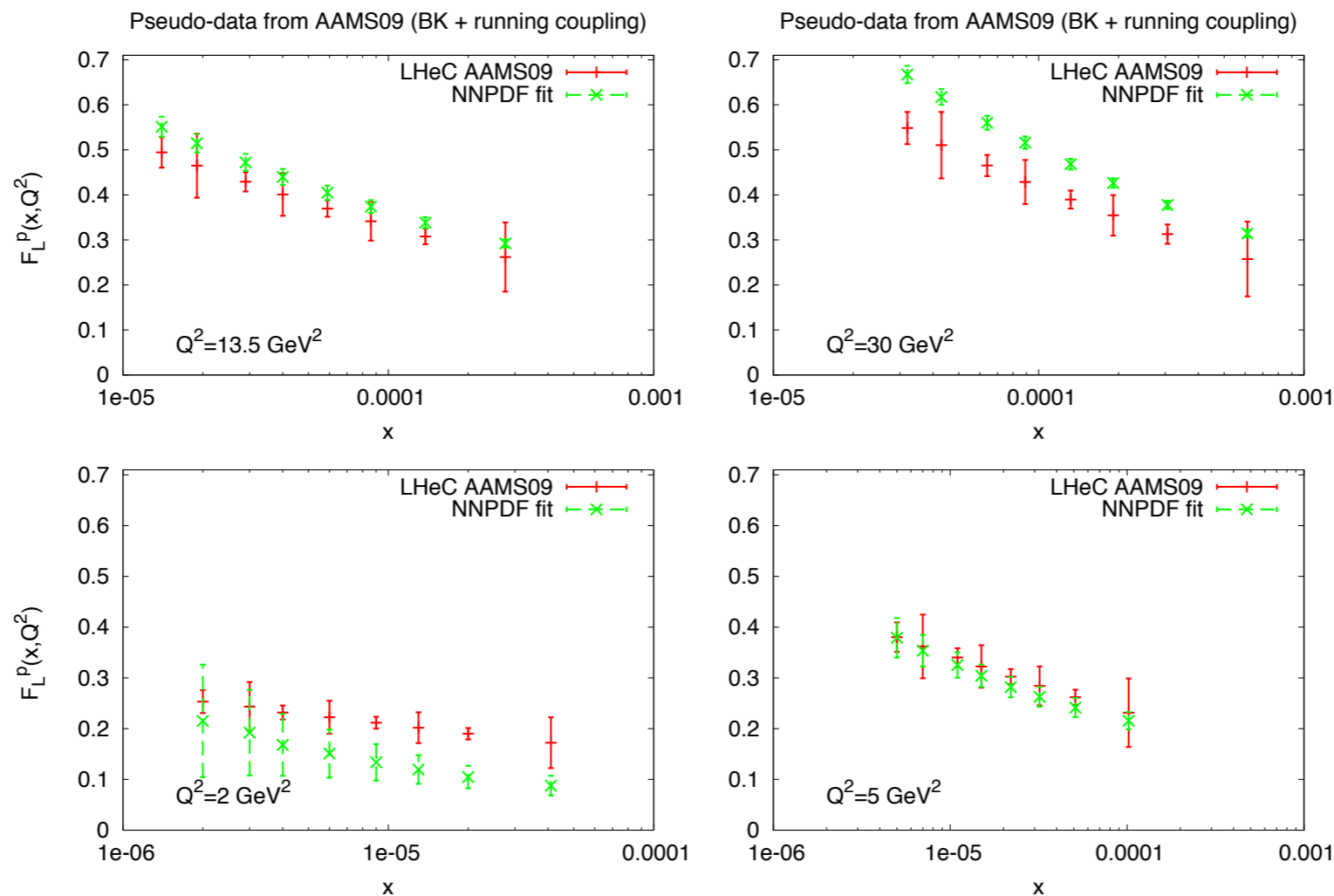

Albacete

Interestingly, rather small band of uncertainties for models based on saturation as compared with the calculations based on the linear evolution. Possible cause: the nonlinear evolution washes out any uncertainties due to the initial conditions, or too constrained parametrization used within the similar framework.

approx. 2% error on the F2 pseudodata, and 8% on the FL pseudodata ,should be able to rule out many of the scenarios.

Testing nonlinear dynamics in ep

Simulated LHeC data using the nonlinear evolution which leads to the parton saturation at low x.
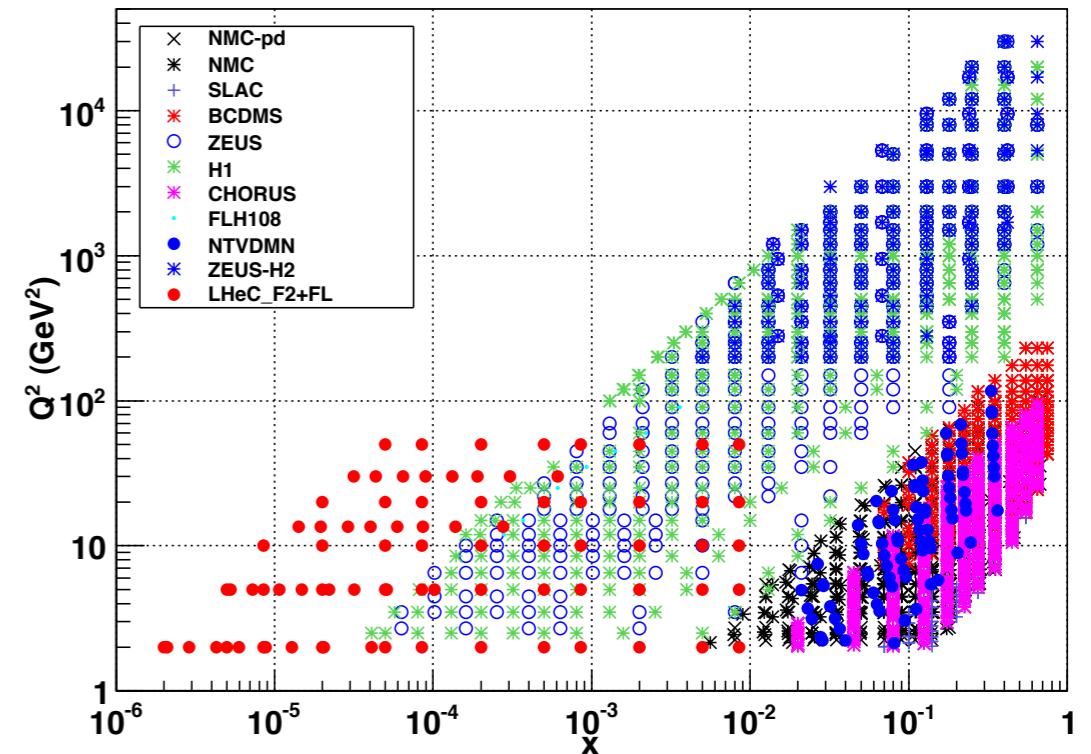
DGLAP fits (using the NNPDF) cannot accommodate the nonlinear effects if F2 and FL are simultaneously fitted.

Albacete,Rojo

FL provides important constraint on the gluon density at low x.
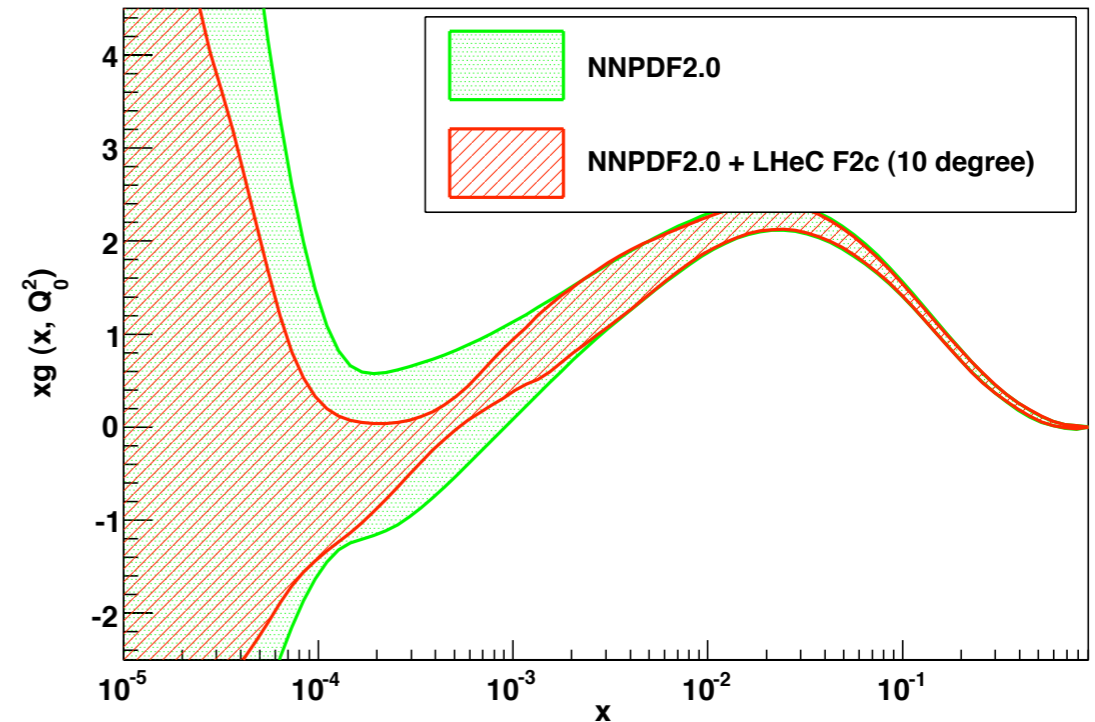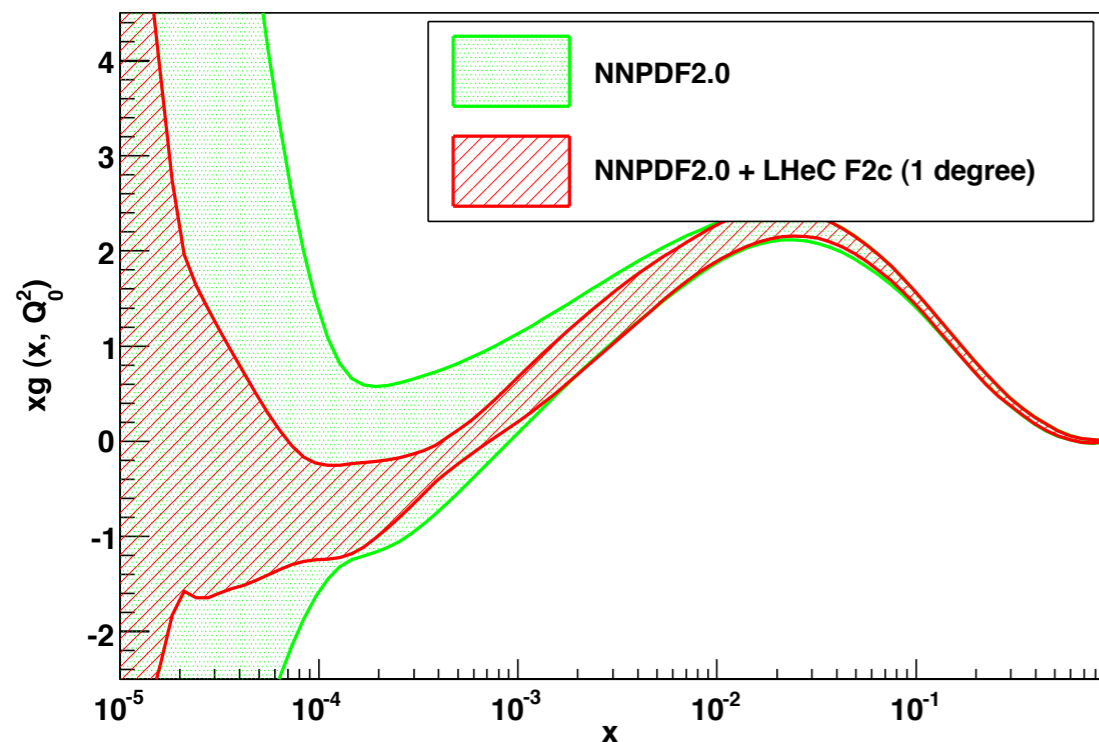
- Inclusion of LHeC pseudodata for F_2, F_L in DGLAP fits improves the determination of the glue at small x.
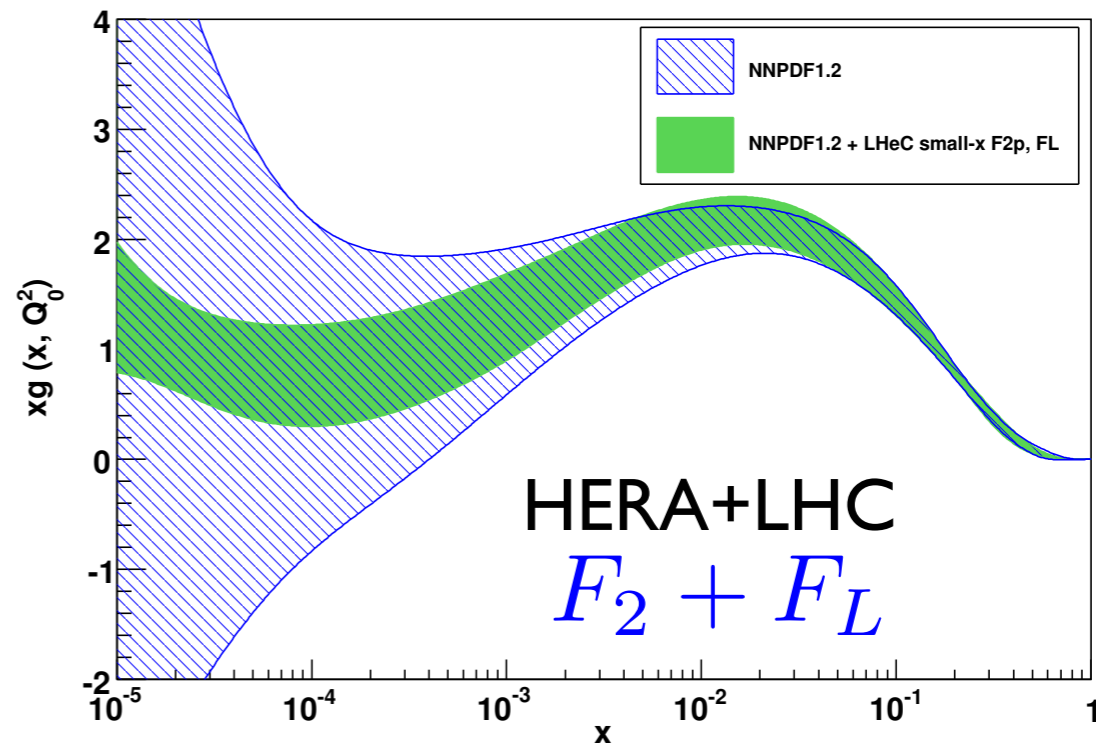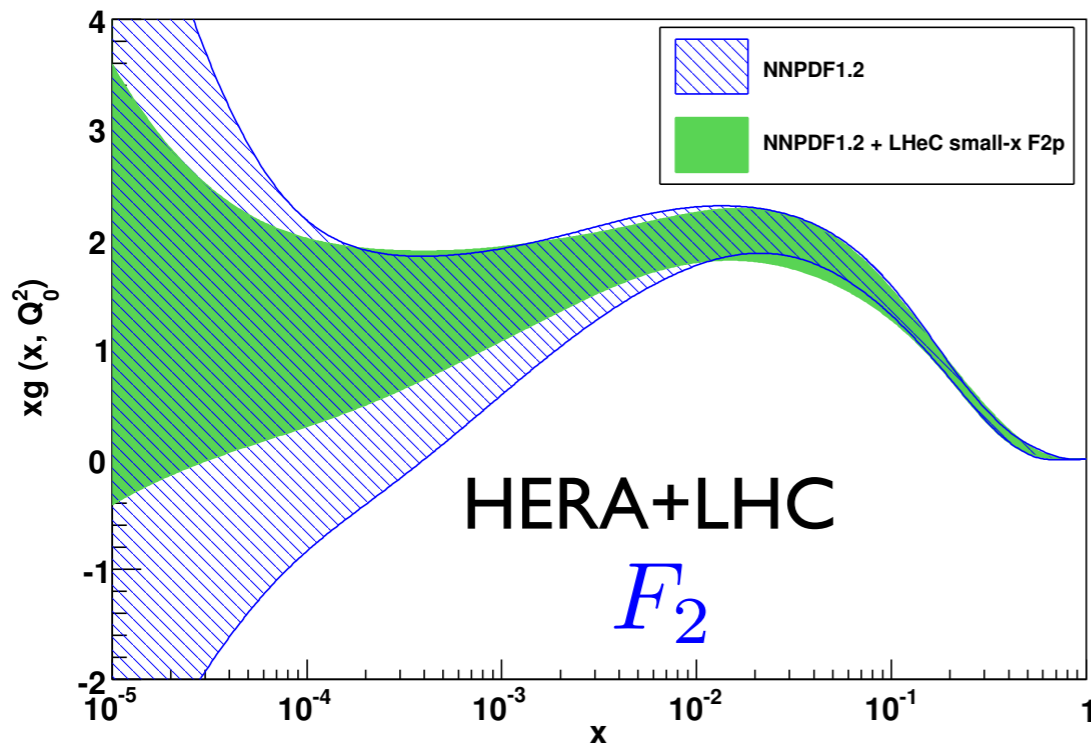
$$Q^2 = 2\ \mathrm{GeV}^2$$

Rojo

Impact of flavor decomposition

Longitudinal structure function difficult to measure. Possibility of using charm structure function to constrain the gluon distribution function.

Rojo

Charm structure function F2c can be used in addition to F2 to constrain the gluon density (red band corresponds to the analysis with the LHeC data on F2charm).

The advantage of 1 degree scenario is also illustrated.

Conclusion: for a better discrimination between models, especially involving nonlinear dynamics, two observables are necessary.
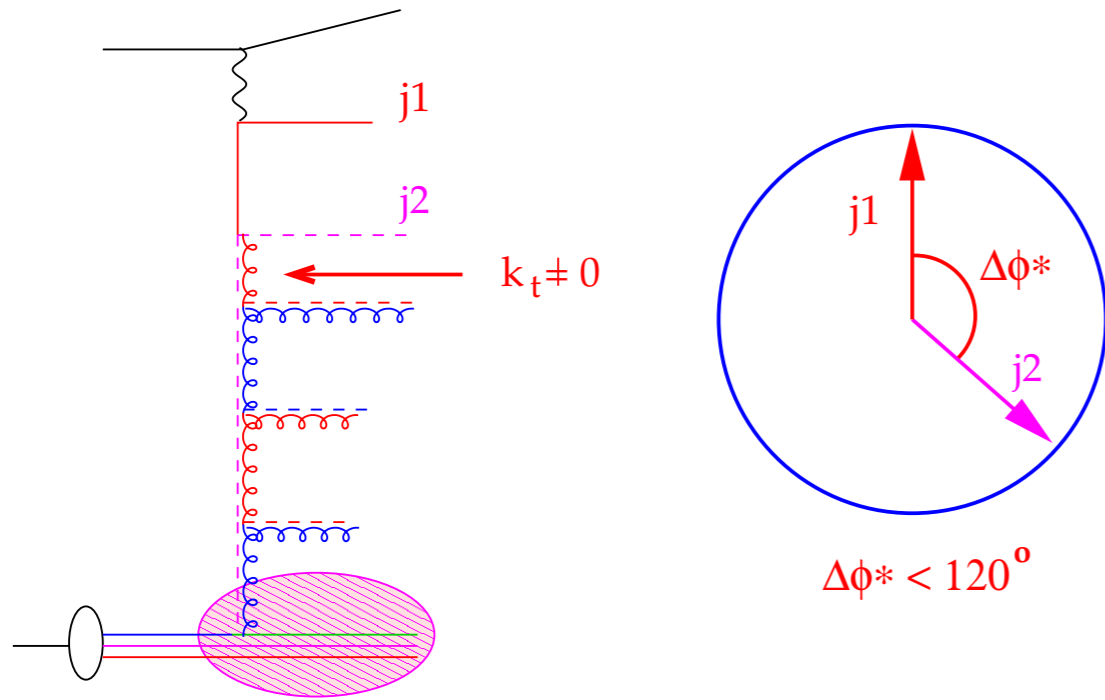
Photoproduction cross section

- Photoproduction cross section.

- Explore dual nature of the photon: pointlike interactions or hadronic behavior.

- Testing universality of hadronic cross sections, unitarity, transition between perturbative and nonperturbative regimes.

- Large divergence of the theoretical predictions beyond HERA measurements.

- Dedicated detectors for small angle scattered electrons at 62m from the interaction point.

- Events with $y \sim 0.3$ $Q^2 \sim 0.01$ could be detected

Pancheri
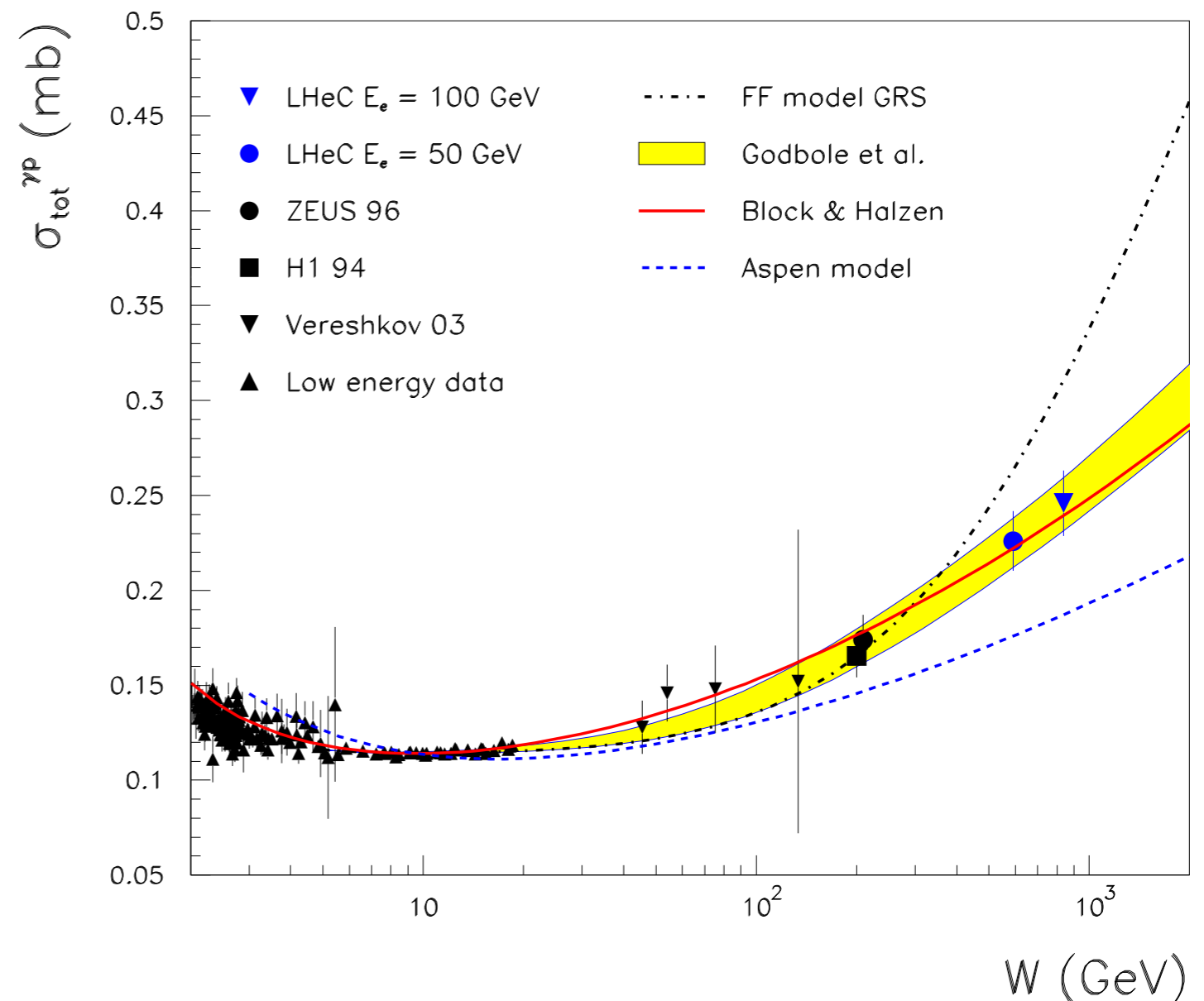
Systematics is the limiting factor here. Assumed 7% for the simulated data as in H1 and ZEUS.

Dijets in ep

- Incoming gluon can have sizeable transverse momentum.
- Decorrelation of pairs of jets, which increases with decreasing value of x.
- Collinear approach typically produces narrow back-to-back configuration. Need to go to higher orders(NLO not sufficient).
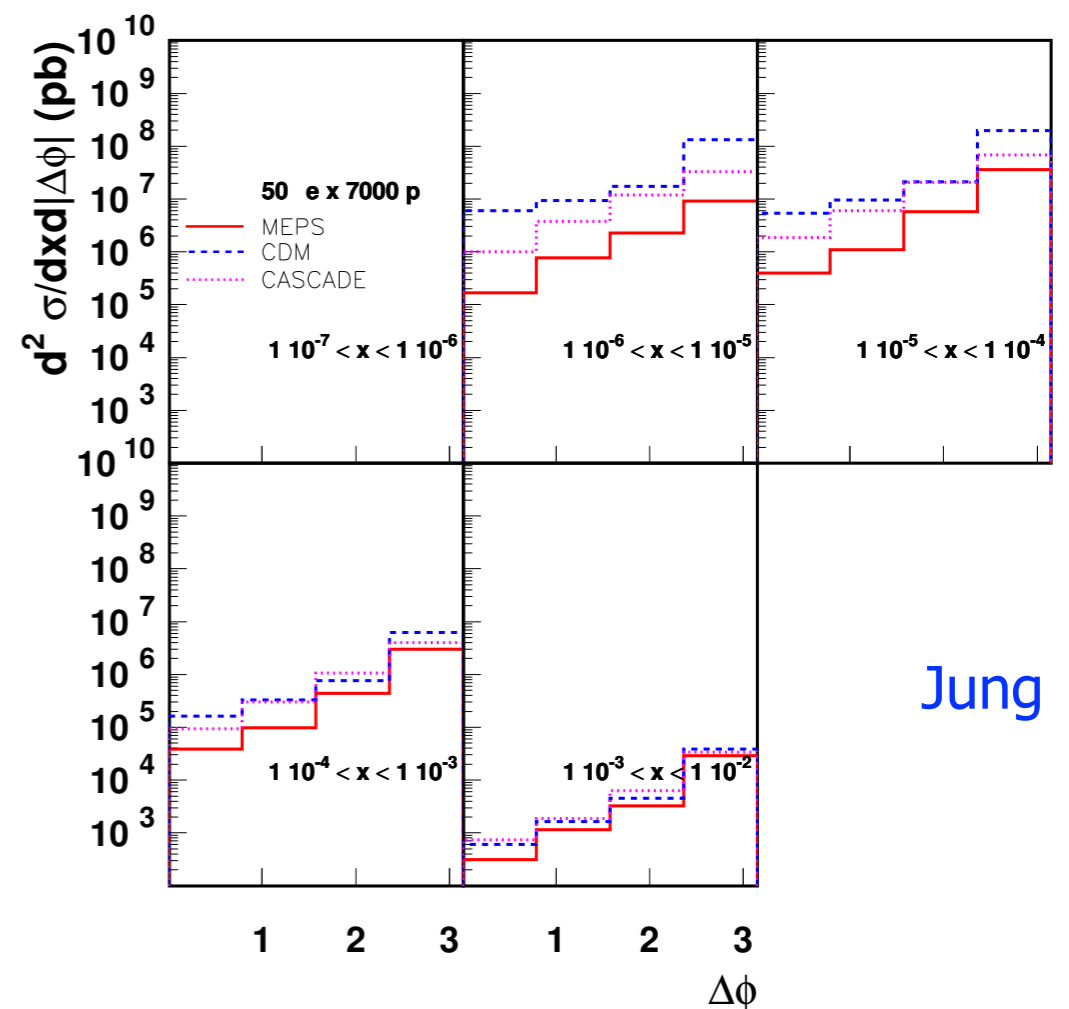
$$-1 < \eta_{\text{jet}} < 2.5 \qquad 0.1 < y < 0.6$$

$$E_{1T} > 7 \text{ GeV} \qquad Q^2 > 5 \text{ GeV}^2$$

$$E_{2T} > 5 \text{ GeV}$$

- All simulations agree at large x.
- CDM, CASCADE give a flatter distribution at small x.

j1
j2
$k_t \neq 0$

$\Delta\phi*$

$\Delta\phi* < 120^{\text{o}}$

Jung
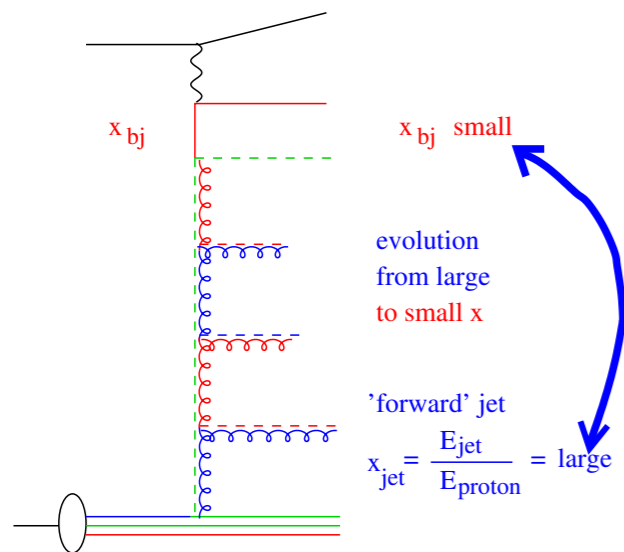
Forward jets

- Forward jet provides the second hard scale.
- By selecting it to be of the order of the photon virtuality, collinear configurations can be suppressed.
- Forward jet, large phase space for gluon emission.
- DGLAP typically underestimates the forward jet production.

x_{bj}

x_{bj} small

evolution from large to small x

'forward' jet

$$x_{jet} = \frac{E_{jet}}{E_{proton}} = \text{large}$$

Simulations for

$$\Theta > 3^o \quad \text{and} \quad \Theta > 1^o$$

Angular acceptance crucial for this measurement.

With $\quad \Theta > 10^o$

all the signal for forward jets is lost.

Can explore also forward pions. Lower rates but no dependencies on the jet algorithms. Non-perturbative hadronisation effects included effectively in the fragmentation functions.
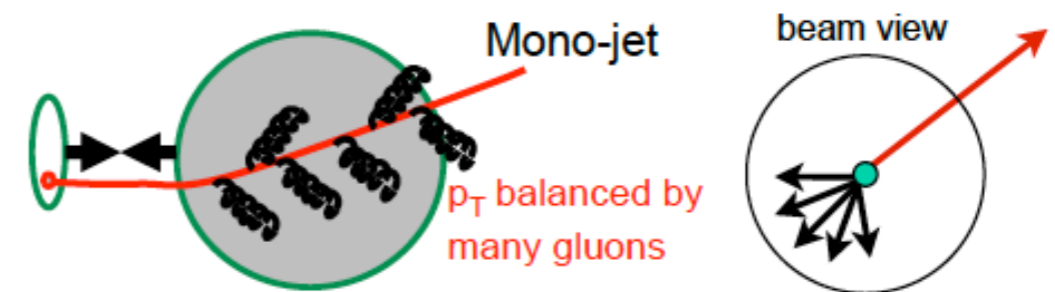
Jung
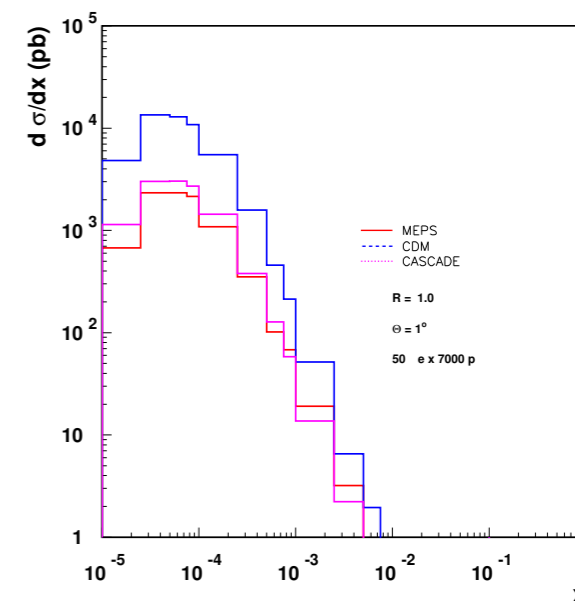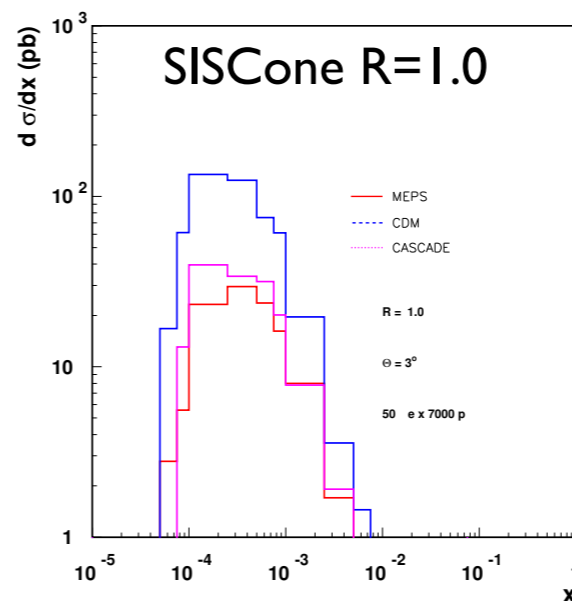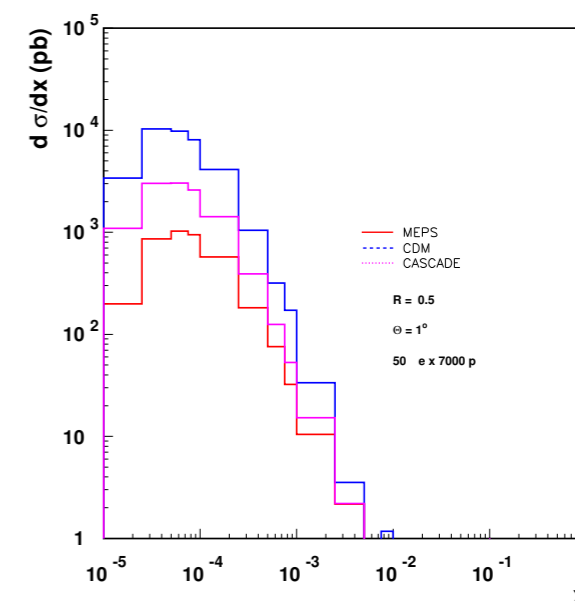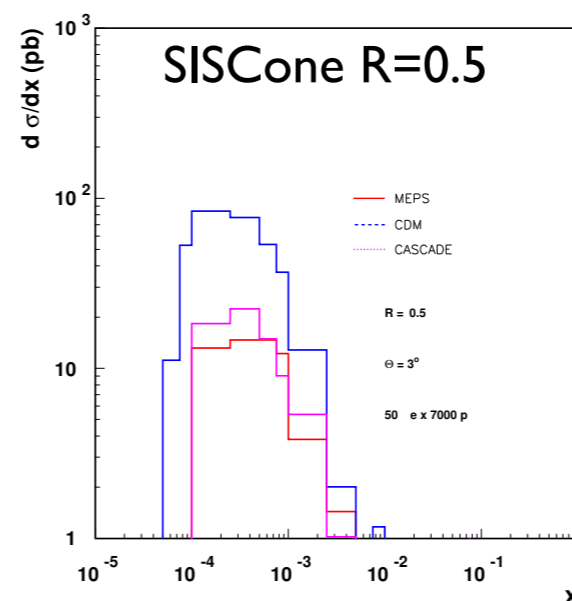
Example: di-hadron correlation in dA collisions

Angular correlation disappears in central dA collisions at forward rapidity
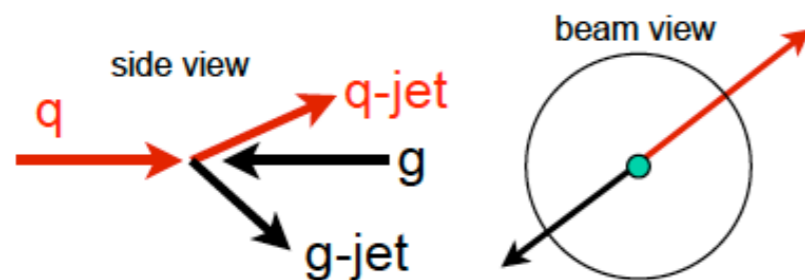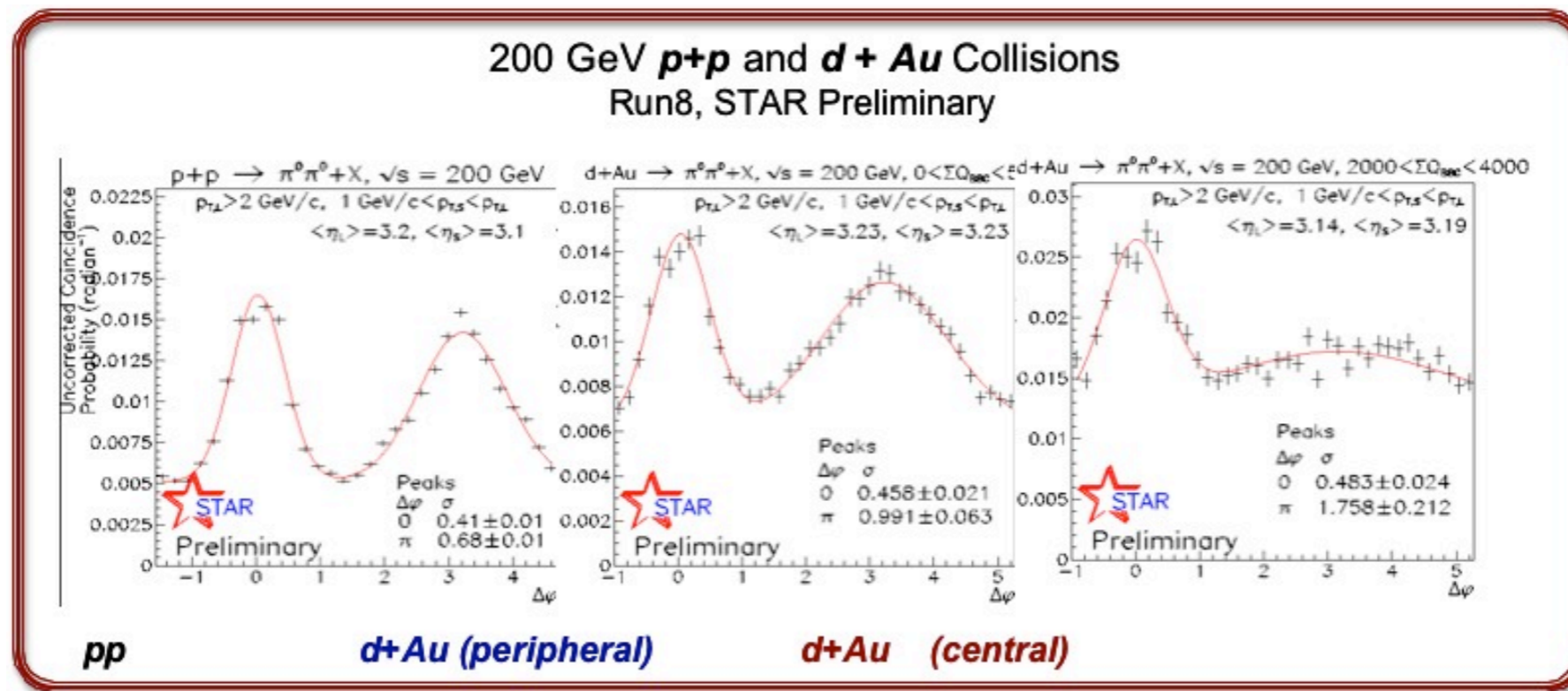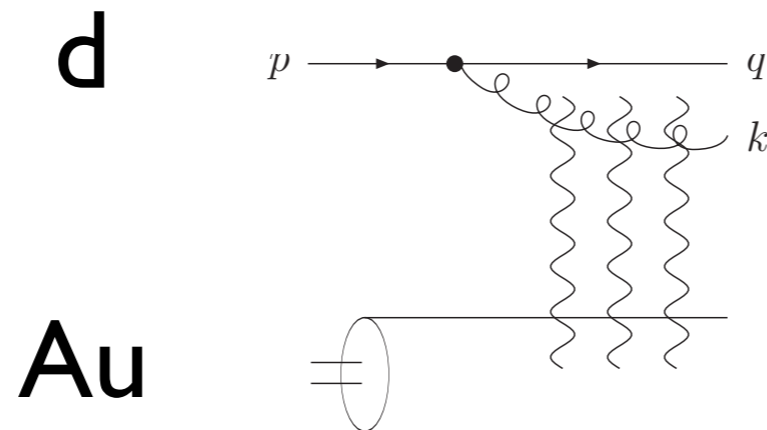

low parton density, back to back configuration

high parton density, multiple rescatterings with heavy nucleus, disappearance of the peak

Example: di-hadron correlation in dA collisions

Naturally explained in the framework of CGC (Color Glass Condensate) via multiple interactions between partons and dense nuclear matter. Albacete & Marquet

In preparation
Yuan ,Xiao, AMS
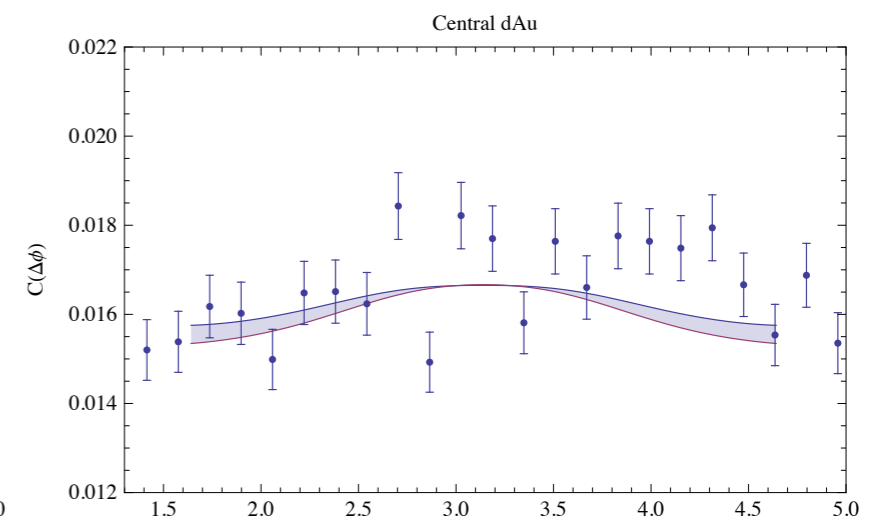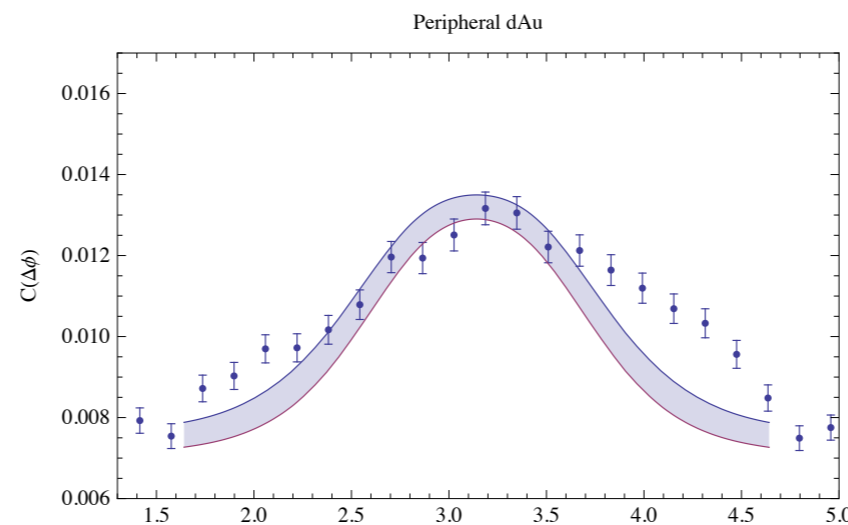
- Necessity of unintegrated/transverse momentum dependent distributions.
- Importance of the 'cold' nuclear matter effects.
- Tests of saturation ideas.
- Ample possibilities of studying variety of processes in DIS in an experimentally cleaner way with a better theoretical control.